

# Four decades of water quality change in the upper San Francisco Estuary

Marcus W. Beck,<sup>\*,†</sup> David Senn,<sup>‡</sup> Thomas Jabusch,<sup>‡</sup> and Phil Trowbridge<sup>‡</sup>

<sup>†</sup>*USEPA National Health and Environmental Effects Research Laboratory, Gulf Ecology Division, Gulf Breeze, FL*

<sup>‡</sup>*San Francisco Estuary Institute, Richmond, CA*

E-mail: [beck.marcus@epa.gov](mailto:beck.marcus@epa.gov)

Phone: +1 (850)9342480. Fax: +1 (850)9342401

## Abstract

Recent methods for trend analysis have been developed that leverage the descriptive potential of long-term time series. Combined with these methods, multi-decadal datasets of water quality in coastal systems can provide valuable opportunities to gain insights into ecosystem properties and drivers of change. This study describes use of an estuarine adaptation of the Weighted Regressions on Time, Discharge, and Season (WRTDS) model to describe water quality trends over four decades in the Delta region of the San Francisco Estuary (SFE). This region is a complex mosaic of inflows that are primary sources of nutrients into the larger Bay. To date, a comprehensive evaluation of flow-normalized trends using the long-term monitoring dataset at multiple stations in the Delta has not been conducted despite the importance of nutrient transport from the region for water quality in the entire bay. The WRTDS technique is data-driven where the parameterization of the functional model changes smoothly over time following dynamic patterns of season and flow. Water quality trends that have not been

{acro:wrtds}

{acro:sfe}

15 previously quantified can be described, including variation in flow-normalized concen-  
16 trations, frequency occurrence of extreme events, and response to historical changes  
17 in the watershed, all of which are important needs for understanding changes in the  
18 SFE. Model results from multiple stations in the Delta provided novel descriptions  
19 of historical trends and relationships between key species of dissolved inorganic nitro-  
20 gen (ammonium, nitrate/nitrite, total). This variation was described in the context of  
21 varying contributions of input flows from the Sacramento and San Joaquin rivers, as  
22 well as tidal exchange with the central SFE. Conceptual relationships between water  
23 quality and drivers of change were used to generate and test hypotheses of mechanistic  
24 relationships using selected examples from the trend descriptions. Overall, this analysis  
25 provides an ecological and management-based understanding of historical trends in the  
26 SFE as a means to interpret potential impacts of recent changes and expected trends in  
27 this dynamic system. An argument is also made for more comprehensive evaluations of  
28 long-term monitoring datasets to understand relationships between response endpoints  
29 and causal mechanisms in coastal waters.

## 30 1 Introduction

31 Trend analysis is a broad discipline that has been applied to time series for the interpretation  
32 of environmentally-relevant changes. Direct evaluation of an observed time series is often  
33 insufficient given that a long-term change can be masked by variation at shorter time scales  
34 or the observed variation represents the combined effects of many variables.<sup>1,2</sup> Climate, local,  
35 regional, and historical effects may act individually or together to impose a change on time  
36 series, such that methods that account for variation at different scales have been used for  
37 trend analysis.<sup>3–6</sup> As a practical approach for water quality evaluation, trend analysis of  
38 eutrophication endpoints often focuses on tracking the change in concentrations or loads of  
39 nutrients over many years. Indicators of eutrophication can vary naturally with variation  
40 in flow conditions and may also reflect long-term effects of management or policy changes.

41 For example, chlorophyll *a* (chl-*a*) concentration as a measure of phytoplankton response {acro:chla}  
42 to nutrient inputs can follow seasonal patterns with cyclical variation in temperature and  
43 light changes throughout each year, whereas annual trends can follow long-term variation  
44 in nutrient inputs to the system.<sup>7,8</sup> Similarly, nutrient trends that vary with hydrologic  
45 loading also vary as a function of utilization rates by primary producers or decomposition  
46 processes.<sup>9–11</sup> Time series analysis of water quality indicators must simultaneously consider  
47 effects of processes at multiple scales and interactions between variables of interest to develop  
48 a more comprehensive description of system change.

49 Appropriate methods for the analysis of change depend largely on the question of inter-  
50 est and on characteristics of the environmental dataset. Trend analyses for aquatic systems  
51 have traditionally focused on comparisons between discrete periods of time to estimate a  
52 direction and magnitude of a trend using non-parametric tests.<sup>12,13</sup> Development of these  
53 conventional approaches addressed limitations in historical monitoring datasets related to  
54 infrequent sampling and relatively few years of continuous data. Increased availability of  
55 multi-decadal datasets, particularly for high profile environments, has accelerated recent de-  
56 velopment of trend analysis methods that leverage the descriptive potential of long-term  
57 time series from continuous monitoring programs.<sup>6,14</sup> These methods are often data-driven  
58 where the parameterization of a simple functional model can change smoothly over time  
59 given that relationships between water quality variables and potential drivers are dynamic.  
60 The Weighted Regressions on Time, Discharge, and Season (WRTDS) approach was devel- {acro:wrtds}  
61 oped under this context and has been used to characterize decadal trends in running-water  
62 systems.<sup>15–19</sup> This method has the potential to provide a spatially and temporally robust  
63 description of trends by fitting a dynamic model with parameters that change relative to the  
64 domain of interest. More recently, the WRTDS method was adapted for trend analysis in  
65 tidal waters, with a focus on chl-*a* trends in Tampa Bay<sup>20</sup> and the Patuxent River Estuary,<sup>21</sup>  
66 and tidally-influenced time series of dissolved oxygen from continuous sonde measurements.<sup>22</sup>  
67 These studies have demonstrated potential for the use WRTDS for trend analysis in tidal

68 waters and further application to alternative datasets could provide additional insight into  
69 drivers of change in aquatic systems.

70 The San Francisco Estuary (SFE) on the Pacific Coast of the United States is one of the {acro:sfe}  
71 most prominent and culturally significant estuaries in the western hemisphere.<sup>23</sup> Background  
72 nutrient concentrations in the Bay often exceed those associated with excessive primary  
73 production, although eutrophication events have historically been infrequent. Recent changes  
74 in response to additional stressors (e.g., variation in freshwater inputs/withdrawals, invasive  
75 species, climate change) suggests that Bay condition has not followed past trajectories and  
76 more subtle spatial and temporal variation could provide clues that describe underlying  
77 properties of this system.<sup>24</sup> The unique ecological and social context of the Bay provides a  
78 valuable opportunity to gain insight into ecosystem properties of estuaries that define water  
79 quality dynamics at different scales. The Delta region of SFE in particular is a mosaic of  
80 inflows that receives and processes inputs from the larger watershed to the lower Bay.<sup>25-27</sup> A  
81 comprehensive monitoring dataset has been collected at several fixed locations in the Delta  
82 for the last four decades.<sup>28</sup> Moreover, nutrient dynamics in the Delta are inherently linked  
83 to flow variation from inputs, withdrawal, impoundments, and downstream transport,<sup>29</sup>  
84 suggesting an approach that explicitly considers flow effects is critical for trend analysis. To  
85 date, the Delta monitoring dataset is an under-utilized data source and a comprehensive  
86 analysis with WRTDS could facilitate an understanding of historical and recent changes in  
87 SFE water quality.

88 The goal of this study was to provide a comprehensive description of nutrient trends in  
89 the Delta to inform understanding of eutrophication dynamics and potential causes of water  
90 quality change in the larger Bay. We applied the newly-adapted method of weighted regres-  
91 sion for tidal waters to describe nitrogen trends in different spatial and temporal contexts.  
92 The specific objectives were to 1) quantify and interpret trends over four decades at ten  
93 stations in the Delta, including annual, seasonal, and spatial changes in nitrogen analytes  
94 and response to flow variation, 2) provide detailed descriptions of two case studies in the

95 context of conceptual relationships modelled with WRTDS. The second objective evaluated  
96 two specific water quality stations in the Delta to demonstrate complexities with nutrient  
97 response to flow, effects of wastewater treatment plant (WWTP) upgrades on water quality,  
98 and effects of biological invasion by benthic filter feeders on primary production. Although  
99 quantitative descriptions of change can be ends in themselves, the results were expected  
100 to have greater impact as a means to more detailed understanding of ecosystem proper-  
101 ties. Products derived from WRTDS can be used to inform additional analyses, such as  
102 water quality response after removing annual, seasonal, or flow effects. Overall, this analysis  
103 is expected to further an ecological and management-based understanding of dynamics in  
104 San Francisco Bay, with implications for water quality restoration and protection of this  
105 prominent system.

## 106 2 Materials and Methods

### 107 2.1 Study system

108 The SFE drains a 200 thousand km<sup>2</sup> watershed and is the largest bay on the Pacific coast of  
109 North America. The watershed provides drinking water to over 25 million people, including  
110 irrigation for 18 thousand km<sup>2</sup> of agricultural land in the Central Valley. Water enters  
111 the Bay through the Sacramento and San Joaquin rivers that have a combined inflow of  
112 approximately 28 km<sup>3</sup> per year, with the Sacramento accounting for 84% of inflow to the  
113 Delta. The SFE system is divided into several sub-bays, including Suisun Bay immediately  
114 downstream of the Delta, San Pablo Bay to the north, South Bay, and the Central Bay  
115 that drains to the Pacific Ocean through the Golden Gate. Water dynamics in SFE are  
116 governed by inflows from the watershed, tidal exchange with the Pacific Ocean, and water  
117 withdrawals for municipal and agricultural use.<sup>25</sup> Seasonally, inflows into SFE peak in the  
118 spring and early summer from snowmelt in the upper watershed, whereas consumption,  
119 withdrawals, and export have steadily increased from 1960 to present but vary considerably

120 depending on inter-annual climate effects.<sup>24</sup> The system is mixed mesotidal and significant  
121 exchange with the ocean occurs daily, although the extent of landward saltwater intrusion  
122 varies with inflow and annual water use patterns. Notable drought periods have occurred  
123 from 1976-1977, 1987-1992, and recently from 2013-2015.<sup>23</sup> Oceanic upwelling and climatic  
124 variation are also significant external factors that have influenced water quality dynamics in  
125 the Bay.<sup>30</sup>

126 Nutrient loading in SFE is comparable to other large estuaries that exhibit symptomatic  
127 effects of cultural eutrophication (e.g., Chesapeake Bay).<sup>31</sup> Orthophosphate ( $\text{PO}_4^{3-}$ ) and {acro:din}  
128 dissolved inorganic nitrogen (DIN) enter the Bay primarily through riverine sources in the  
129 north and municipal WWTP inputs in the densely-populated area immediately surrounding  
130 SFE. Annual nutrient export from the Delta region has been estimated as approximately 30  
131 thousand kg d<sup>-1</sup> of total nitrogen (varying with flow<sup>29</sup>), with 90% of ammonium ( $\text{NH}_4^+$ ) orig-  
132 inating solely from the Sacramento Regional WWTP.<sup>27</sup> Although nitrogen and phosphorus  
133 inputs are considerable, primary production is relatively low and not nutrient-limited.<sup>26,32</sup>  
134 The resistance of SFE to the negative effects of eutrophication has historically been at-  
135 tributed to the unique physical and biological characteristics of the Bay, including strong  
136 tidal mixing that limits stratification<sup>7,33</sup> and limits on phytoplankton growth from high tur-  
137 bidity and filter-feeding by bivalve mollusks.<sup>33,34</sup> However, recent water quality trends have  
138 suggested that resistance of the system to nutrient inputs is decreasing given documented  
139 changes in chlorophyll biomass,<sup>30</sup> increased occurrence of hypoxic conditions,<sup>35</sup> and increased  
140 abundance of phytoplankton species associated with harmful algal blooms.<sup>36,37</sup> These recent  
141 changes have been attributed to variation in global sea surface temperatures associated with  
142 climate change,<sup>30</sup> biological invasions,<sup>38</sup> and departures from the historical flow record.<sup>24,39</sup>  
143 The role of nutrients in stimulating primary production in SFE has been the focus of several  
144 recent investigations.<sup>40-42</sup>

145 The Delta region is of particular interest for understanding historical patterns and po-  
146 tential trajectories of water quality response to nutrient inputs into the Bay (Figure 1). The

<sup>147</sup> Delta is a mosaic of linked channels or tracts that receive, process, and transport inflows  
<sup>148</sup> from the Sacramento and San Joaquin rivers.<sup>25,27,29</sup> Quantitative descriptions of nutrient  
<sup>149</sup> dynamics in the Delta are challenging given many nutrients sources and the volume of water  
<sup>150</sup> that is exchanged through the system with natural and anthropogenic processes. A com-  
<sup>151</sup> prehensive evaluation using mass-balance models to describe nutrient dynamics in the Delta  
<sup>152</sup> demonstrated that nitrogen enters the system in different forms and is processed at differ-  
<sup>153</sup> ent rates before export or removal.<sup>29</sup> For example, a majority of ammonium entering the  
<sup>154</sup> system during the summer is nitrified or assimilated, whereas a considerable percentage of  
<sup>155</sup> total nitrogen load to the Delta is lost. Although, the focus of our analysis is not to quan-  
<sup>156</sup> tify sources or sinks of nitrogen species, a quantitative evaluation of long-term trends will  
<sup>157</sup> provide a more comprehensive historical interpretation to hypothesize the effects of future  
<sup>158</sup> changes in the context of known dynamics. Nutrients in the Delta also vary with seasonal  
<sup>159</sup> and annual changes in the delivery of water inflows, including water exports directly from the  
<sup>160</sup> system.<sup>25,27</sup> Our analysis also explicitly accounts for the effects of flow changes on nutrient  
<sup>161</sup> response to better understand variation both within the Delta and potential mechanisms of  
<sup>162</sup> downstream transport.

## <sup>163</sup> 2.2 Data sources

<sup>164</sup> Multi-decadal time series of nutrients and flow records were used to develop a quantitative  
<sup>165</sup> description of nitrogen trends in the Delta. The Interagency Ecological Program (IEP) is a {acro:iep}  
<sup>166</sup> consortium of state and federal agencies that have maintained the Environmental Monitoring {acro:emp}  
<sup>167</sup> Program (EMP) in the Delta region since 1975.<sup>43</sup> The EMP collects monthly water quality  
<sup>168</sup> samples at 19 stations in the Delta, Suisun Bay, and northeastern San Pablo Bay. Water  
<sup>169</sup> samples were collected using a Van Dorn sample, a submersible pump, or a flow through sys-  
<sup>170</sup> tem depending on site. All samples were processed with standard QA/QC at the California  
<sup>171</sup> Department of Water Resources Bryte Laboratory in Sacramento.<sup>43</sup> Nutrient time series were  
<sup>172</sup> obtained from the IEP website (<http://water.ca.gov/bdma/meta/Discrete/data.cfm>) at

<sup>173</sup> ten discrete sampling stations from 1976 through 2013 (Figure 1). Stations were grouped  
<sup>174</sup> by location in the study area for comparison: Delta stations C3 (Sacramento inflow), C10  
<sup>175</sup> (San Joaquin inflow), MD10, P8; middle stations D19, D26, D28; and Suisun stations D4,  
<sup>176</sup> D6, and D7. These stations were chosen based on continuity of the water quality time series  
<sup>177</sup> and geographic location for understanding trends. Time series were complete for all stations  
<sup>178</sup> except for an approximate ten year gap from 1996-2014 for D19. Data were minimally pro-  
<sup>179</sup> cessed with the exception of averaging replicates that occurred on the same day. The three  
<sup>180</sup> nitrogen analytes that were evaluated were ammonium, nitrite/nitrate, and DIN (as the sum  
<sup>181</sup> of the former two). Less than 3% of all observations were left-censored, although variation  
<sup>182</sup> was observed between analytes and location. The most censored observations were observed  
<sup>183</sup> for ammonium time series at sites C10 (25.4%), D28 (17.8%), D19 (12%), D7 (7.9%), and  
<sup>184</sup> D4 (6.4%).

<sup>185</sup> Daily flow estimates for the Delta region were obtained from the Dayflow software pro-  
<sup>186</sup> gram that provides estimates of average Delta outflow.<sup>44</sup> Because of the complexity of water  
<sup>187</sup> inflow, exports, and outflows from the Delta, the Dayflow program combines observations  
<sup>188</sup> with estimates based on mass balance to reconstruct historical and daily flow estimates.  
<sup>189</sup> The WRTDS models described below require a matched flow record with the appropriate  
<sup>190</sup> station to evaluate nutrient trends. Given the complexity of inflows and connectivity of the  
<sup>191</sup> system, only the inflow estimates from the Sacramento and San Joaquin rivers were used as  
<sup>192</sup> measures of freshwater influence at each station. Initial analyses indicated that model fit  
<sup>193</sup> was not significantly improved with flow estimates from locations closer to each station, nor  
<sup>194</sup> was model fit improved using lagged times series. As such, the Sacramento daily flow time  
<sup>195</sup> series was used to account for flow effects at C3, D19, D26, and D28, and the San Joaquin  
<sup>196</sup> time series was used for C10 and P8. The salinity observations at D4, D6, and D7 in Suisun  
<sup>197</sup> Bay were used as a more appropriate measure of variation in freshwater balance given the  
<sup>198</sup> stronger tidal influence at these stations. Salinity has been used as a tracer of freshwater  
<sup>199</sup> influence for the application of WRTDS models in tidal waters.<sup>20</sup>

200 2.3 Analysis method and application

201 A total of thirty WRTDS models were created, one for each nitrogen analyte at each station.  
202 The functional form of WRTDS is a simple regression<sup>15</sup> that models the log-transformed  
203 response variable as a function of time, flow, and season:

$$\ln(N) = \beta_0 + \beta_1 t + \beta_2 \ln(Q) + \beta_3 \sin(2\pi t) + \beta_4 \cos(2\pi t) \quad (1)$$

204 where  $N$  is one of three nitrogen analytes, time  $t$  is a continuous variable as decimal time  
205 to capture the annual or seasonal trend, and  $Q$  is the flow variable (either flow or salinity  
206 depending on station). The seasonal trend is modelled as a sinusoidal component to capture  
207 periodicity between years. The WRTDS model is a moving window regression that fits  
208 a unique set of parameters at each observation point in the time series. A unique set of  
209 weights is used for each regression to control the relevance of observations used to fit the  
210 model to the observation at the center of the window. The weights are based on a scaled  
211 Euclidean distance to estimate the differences of all points from the center in relation to  
212 annual time, season, and flow. The final vector used to fit the model at each point weights  
213 observations more similar to the center of the window with more importance. The complete  
214 model for the time series contains a parameter set for every time step that considers the  
215 unique context of the data. As such, predictions from WRTDS are more precise than those  
216 from more conventional models that fit a single parameter set to the entire time series.<sup>20,45</sup>  
217 The WRTDS model applied to the Delta time series was based on a tidal adaptation of the  
218 original method.<sup>20</sup> The WRTDS models were fit to describe the conditional mean response  
219 using a weighted Tobit model for left-censored data.<sup>46</sup> Previous adaptations of WRTDS to  
220 tidal waters have used quantile regression to describe trends in the conditional quantiles,  
221 such as changes in the frequency of occurrence of extreme events. The application to the  
222 Delta data focused only on the conditional mean models to establish a baseline response  
223 which has not been previously quantified. All analyses used the WRTDStidal package for

<sup>224</sup> R.<sup>47,48</sup>

<sup>225</sup> A hallmark of the WRTDS approach is the description of flow-normalized trends that  
<sup>226</sup> are independent of variation from freshwater inflows. Flow-normalized trends have value for  
<sup>227</sup> the interpretation of changes that are potentially caused by drivers other than flow, such as  
<sup>228</sup> WWTP upgrades or phytoplankton grazing by benthic filter-feeders.<sup>20</sup> Although variation  
<sup>229</sup> in nutrients is caused by the combined effects of several variables acting at different temporal  
<sup>230</sup> and spatial scales, flow-normalization provides a basis for further exploration by removing a  
<sup>231</sup> critical confounding variable that could affect the interpretation of trends. A flow-normalized  
<sup>232</sup> value is the average of predictions at a given observation using all flow values that are ex-  
<sup>233</sup> pected to occur for the relevant month across years in the record. Flow-normalized trends for  
<sup>234</sup> each analyte at each station were used to describe long-term changes in different annual and  
<sup>235</sup> seasonal periods. Specifically, flow-normalized trends in each analyte were summarized as  
<sup>236</sup> both medians and percent changes from the beginning to end of annual groupings from 1976-  
<sup>237</sup> 1995 and 1996-2013, and seasonal groupings of March-April-May (spring), June-July-August  
<sup>238</sup> (summer), September-October-November (fall), and December-January-February (winter)  
<sup>239</sup> within each annual grouping. These annual and seasonal groupings were chosen for conti-  
<sup>240</sup> nuity with similar comparisons reported in Ref. 28 and as approximate twenty year midway  
<sup>241</sup> points in the time series.

<sup>242</sup> Trends within each annual and seasonal grouping were based on seasonal Kendall tests of  
<sup>243</sup> the flow-normalized predictions. This test is a modification of the non-parametric Kendall  
<sup>244</sup> test that accounts for variation across seasons in the response variable.<sup>49</sup> Results from the  
<sup>245</sup> test can be used to evaluate the direction, magnitude, and significance of a monotonic change  
<sup>246</sup> within the period of observation. The estimated rate of change per year is also returned as  
<sup>247</sup> the Theil-Sen slope and was interpreted as the percent change per year when divided by the  
<sup>248</sup> median value of the response variable in the period of observation.<sup>27</sup> Trends within annual  
<sup>249</sup> groupings were based on all monthly observations within relevant years, whereas seasonal  
<sup>250</sup> groupings were based only on the relevant months across years. Seasonal Kendall tests were

251 also used to describe trends in the model predictions for the observed data. These trends were  
252 compared with those based on the flow-normalized trends to evaluate the improved ability of  
253 WRTDS to describe trends that are independent of flow. Functions in the EnvStats package  
254 in R were used for the seasonal Kendall tests.<sup>50</sup>

## 255 3 Results and Discussion

### 256 3.1 Observed Data

257 The observed time series for the ten Delta stations had substantial variation in scale among  
258 the nitrogen analytes and differences in apparent seasonal trends (Figure 2). In general,  
259 long-term (inter-annual) trends were not easily observed from the raw data. Total DIN for  
260 most stations was dominated by nitrite/nitrate, whereas ammonium was a smaller percent-  
261 age of the total. However, C3 had a majority of DIN composed of ammonium and other  
262 stations (e.g., P8, D16) had higher concentrations of ammonium during winter months when  
263 phytoplankton assimilation is lower.<sup>7</sup> By location, observed concentrations of DIN for the  
264 entire time series were higher on average for the upper Delta stations (C3, C10, MD10, P8;  
265 maximum likelihood estimation of mean  $\pm$  standard error:  $1.16 \pm 0.03 \text{ mg L}^{-1}$ ) and similar for  
266 the middle (D19, D26, D28,  $0.43 \pm 0.01$ ) and Suisuan Bay stations (D4, D6, D7,  $0.44 \pm 0.01$ ).  
267 Average concentrations were highest at P8 ( $1.63 \pm 0.05 \text{ mg L}^{-1}$ ) and lowest at C3 ( $0.4 \pm 0.01$ )  
268 for DIN, highest at P8 ( $0.28 \pm 0.02$ ) and lowest at D28 ( $0.05 \pm 0.003$ ) for ammonium, and  
269 highest at C10 ( $1.4 \pm 0.04$ ) and lowest at C3 ( $0.15 \pm 0.004$ ) for nitrite/nitrate. Mean observed  
270 concentrations were also higher later in the time series for all analytes. For example, av-  
271 erage DIN across all stations was  $0.62 \pm 0.01 \text{ mg L}^{-1}$  for 1976-1995, compared to  $0.72 \pm 0.01$   
272 for 1996-2013. Seasonal changes across all years also suggested that nitrogen concentrations  
273 were lower in the summer and higher in the winter. However, observed seasonality patterns  
274 were inconsistent between sites. For example, site MD10 had distinct seasonal spikes for  
275 elevated DIN in the winter, whereas other stations had less prominent variation between

<sup>276</sup> years (D6, D7, Figure 2).

## <sup>277</sup> 3.2 Trends

<sup>278</sup> Application of seasonal Kendall tests to evaluate trends in observed data provided explicit in-  
<sup>279</sup> formation on the direction, magnitude, and statistical significance of changes between years.  
<sup>280</sup> Trends estimated from the observed data for 1976-1995 and 1996-2013 varied considerably  
<sup>281</sup> between sites and analytes (Figure 3). Significant trends were observed from 1976-1995 for  
<sup>282</sup> eight of ten sites for DIN (seven increasing, one decreasing), eight sites for ammonium (six  
<sup>283</sup> increasing, two decreasing), and six sites for nitrite/nitrate (five increasing, one decreasing).  
<sup>284</sup> More sites had decreasing trends for the observed data from 1996-2013. Eight sites had  
<sup>285</sup> significant trends for DIN (four increasing, four decreasing), seven sites for ammonium (five  
<sup>286</sup> increasing, two decreasing), and eight sites for nitrite/nitrate (four increasing, four decreas-  
<sup>287</sup> ing). Trends by location (upper Delta, middle, and Suisun stations) were not apparent,  
<sup>288</sup> suggesting individual sites had trends that differed independent of relative location. For  
<sup>289</sup> example, P8 had a relatively large decrease in ammonium (-8.3% change per year) for the  
<sup>290</sup> second annual period compared to all other sites. Trends by season were similar such that  
<sup>291</sup> increases were generally observed in all seasons for the first time period from 1976-1995 and  
<sup>292</sup> decreases were observed for the second (Figures S1 and S2), although trends were noisier  
<sup>293</sup> and significant changes were less common compared to the annual comparisons.

<sup>294</sup> Relationships between flow and observed water quality are complex and can change signif-  
<sup>295</sup> icantly through space and time.<sup>15,19</sup> These principles have been demonstrated for monitoring  
<sup>296</sup> data in the Delta region,<sup>27-29</sup> suggesting that trend analyses using the observed time series  
<sup>297</sup> are potentially confounded by flow effects. A simple monotonic change over time could re-  
<sup>298</sup> flect mobilization or dilution effect of flow rather than a response to nutrient sources. As a  
<sup>299</sup> proof of concept, Figure 4 demonstrates use of WRTDS to isolate a flow-normalized time  
<sup>300</sup> series from the observed data. The raw data are presented in Figure 4a and the annual  
<sup>301</sup> predicted and flow-normalized results from WRTDS are shown in Figure 4b.

302 Emphasize the information the model provides relative to the observed time series. A  
303 distinct annual trend with a maximum in the middle of the time series is observed, with lower  
304 values at the beginning and end of the period. The seasonal patterns generally showed that  
305 DIN concentrations were highest in January with higher values at moderate to low flow rates  
306 depending on the year. Interestingly, summer and fall concentrations have showed a slight  
307 increase later in the time series ( 2004-2009). The confounding effect of flow is also very  
308 apparent such that higher flows were associated with lower concentration. Dynaplot showed  
309 that there was always a negative association between the two (i.e., no modal response).  
310 Emphasize the summer/fall change in the 2000s, why is this? Check,<sup>30</sup> showed seasonal  
311 changes in early 2000s in chlorophyll (NE Pacific shifted to cool phase), is there a mechanism  
312 here with DIN? Relate to conceptual diagram.

313 Effects of flow on trend interpretation shown in Figures S1 to 3.

### 314 3.3 Selected examples

315 Two stations were chosen for closer evaluation to demonstrate use of WRTDS to develop a  
316 more comprehensive description of decadal trends in the Delta. The stations were chosen to  
317 address ecological and management-based questions that have relevance outside of the region,  
318 having importance for the understanding of estuarine processes that influence eutrophication  
319 trends over several years. The selected case studies focused on 1) effects of wastewater  
320 treatment upgrades upstream of P8, and 2) effects of biological invasion on nutrient dynamics  
321 in Suisun Bay. Each case study is built around hypotheses that results from WRTDS models  
322 were expected to support, both as a general description and for additional testing with  
323 alternative methods.

#### 324 3.3.1 Effects of wastewater treatment

325 Wastewater treatment plants upstream of and within the Delta are a major source of nutrient  
326 loading to the system. As noted in,<sup>27</sup> the Sacramento Regional WWTP alone contributes

327 90% of the ammonium load to the region. Significant efforts have been made in recent years  
328 to reduce nitrogen loading from regional WWTPs given the disproportionate contribution  
329 of nutrients relative to other sources (e.g., watershed agricultural load, sediment flux, etc.,  
330 ).<sup>29,51</sup> Several WWTPs have recently been or are planned to be upgraded to include tertiary  
331 filtration and nitrification to convert biologically available ammonium to nitrate. The City  
332 of Stockton WWTP was upgraded in 2006 and is immediately upstream of station P8.<sup>28</sup>  
333 Therefore, a modal response of nutrient concentrations at P8 centered around 2006 is ex-  
334 pected as a result of upstream WWTP upgrades, and water quality should exhibit 1) a  
335 shift in load contributions before/after upgrade, 2) a flow-normalized annual trend at P8  
336 to show a change concurrent with WWTP upgrades, and 3) different nitrogen species will  
337 have different changes depending on change in load outputs. The use of WRTDS to describe  
338 downstream effects of WWTP upgrades could reveal flow-independent trends that have not  
339 been previously described.

340 Overall reduction in total nitrogen load was observed as a result of reduction in ammo-  
341 nium (Figure S3). Nitrate is the primary constituent of total nitrogen after 2007. Organic  
342 nitrogen is a larger percentage of the total after nitrification. What was reduction in ammo-  
343 nium starting in 2002?

344 Nitrogen trends at P8 shifted in response to upstream WWTP upgrades (Figure 6), with  
345 ammonium showing the largest reduction. Interestingly, nitrite/nitrate concentrations also  
346 showed a similar but less dramatic decrease. Percent changes are shown in Table 4, where  
347 both nitrogen species shows large percent increases prior to WWTP upgrades followed by de-  
348 creases after upgrades with ammonium showing the largest pecentage. Seasonally, increases  
349 prior to upgrades were most apparent in the July-August-September (JAS) months for both {acro:jas}  
350 analytes. Seasonal reductions post-upgrades were also largest in JAS for nitrite/nitrate,  
351 whereas percent reductions were similar across all monthly groupings for ammonium.

352 Relationships of nitrogen with flow showed the typical inverse flow/concentration dynamic  
353 with flushing at high flow, although patterns differed by nitrogen species. Seasonal variation

354 was more apparent for ammonium, although both typically had the highest concentrations  
355 in the winter. Additionally, strength of the flow/nutrient relationship changed throughout  
356 the time series the year where the strongest relationship differed by analyte. Nitrite/nitrate  
357 typically had the strongest relationship flow later in the time series, whereas ammonium had  
358 the strongest relationship with flow in the early 2000s.

359 **3.3.2 Effects of biological invasions**

360 The San Francisco Estuary is considered one of the most invaded ecosystems in the world  
361 with an estimated 234 exotic species by the turn of the century, half of which have been  
362 reported after 1965.<sup>38</sup> The invasion of benthic grazers as ecosystem engineers is one of the  
363 more notable events that has been characterized by dramatic shifts in primary production  
364 of the Bay's trophic network.<sup>34,52-54</sup> In particular, invasion of the upper estuary by the  
365 Asian clam *Potamocorbula amurensis* in 1986 caused dramatic changes in phytoplankton  
366 abundance and species composition with increased grazing. Reduction in phytoplankton  
367 biomass has altered trophic networks in the Bay and is considered a primary mechanism in  
368 the decline of the protected delta smelt and other important fisheries.<sup>55,56</sup> Changes in the  
369 physical environment have also occurred with the most notable effect being increased water  
370 clarity following a reduction of phytoplankton.<sup>56</sup> The clams are halophilic such that drought  
371 years are generally correlated with an increase in biomass and further upstream invasion of  
372 the species.<sup>24,57</sup>

373 We hypothesized that WRTDS models applied to water quality observations in the up-  
374 per estuary would show 1) a decline in annual, flow-normalized chlorophyll concentrations  
375 over time coincident with an increase in abundance of invaders, 2) changes in ratios of lim-  
376 iting nutrients (nitrogen, SiO<sub>2</sub>) suggesting different uptake rates by grazers with a shift in  
377 community composition, and 3) seasonal shifts in limiting nutrients based on changes in  
378 community composition and relative abundances with seasonal succession. The application  
379 of WRTDS to water quality observations at station D7 in Suisun Bay and comparison with

380 clam abundance and biomass data from<sup>34</sup> was expected to reveal the competing effects of  
381 inflow on phytoplankton and benthic grazers.

382 Data from<sup>27,34</sup> describes phytoplankton community changes in the upper estuary, includ-  
383 ing chlorophyll response to flow. Figure 10 in Ref. 27 showed that chlorophyll generally  
384 decreased with flow in 1980 but increased with flow in 2000.

385 Note the decrease in Potamocorbula abundance in 2011, 2012. These are wet years where  
386 abundance/biomass of the clams is driven down by lower salinity. Contrased wtih the annual  
387 chlorophyll trends in the same years, the predicted values are above the flow-normalized trend  
388 suggesting an increase in chlorophyll with higher flow. The potential mechanism is therefore  
389 a decrease in clam abundance with high flow that releases phytoplankton from filtration  
390 pressure. This also explains the positive association of chlorophyll with flow in recent years  
391 (bottom right dynaplot). See suggestions in Ref. 57,58 regarding flow/grazer relationships  
392 in the Bay.

393 Further, chlorophyll trends early in the time series generally show a decrease with high  
394 flow with a distinct maximum at moderate flow. This may suggest stratification events  
395 at moderate flow contributed to phytoplankton blooms early in the time series. Water  
396 withdrawals later in the time series could have also altered environmental conditions to  
397 reduce the frequency occurrence of stratification events. Look into this more...

398 What about biomass/density relationships for Potamocorbula? Although clam density  
399 increases throughout the period, What about initial decrease in chlorophyll prior to clam  
400 invasion? Is this related to water withdrawals (i.e., decrease in stratification events at mod-  
401 erate flow)?

402 Figure 7, Table 5

#### 403 3.4 Implications

404 Implications of different flow varialbes - refer to,<sup>29</sup> a hybrid approach would be best for  
405 complex systems like the delta.

406 Second case study showed typical inverse relationships between nutrients and flow, more  
407 flow means greater flushing and dilution of nutrient concentrations. Conversely, low flow  
408 means less flushing and higher nutrient concentrations, although this may not always be  
409 observed if the available nutrients are biologically available. Low-flow events during warmer  
410 months show the lowest ammonium concentrations, which corresponds to seasonal max-  
411 ima in chlorophyll concentration. A similar but weaker relationship was observed with  
412 nitrite/nitrate where increased flow was related to decreased concentration and lower con-  
413 centrations overall were observed in the summer. However, low-flow events still had higher  
414 concentrations than high-flow events in July, as compared to ammonium which was low re-  
415 gardless of flow. This suggests that ammonium concentrations are driving phytoplankton  
416 production at P8. Annual trends in chlorophyll concentration (not shown) showed an overall  
417 decrease from the 1970s to present, although a slight peak is observed in the 2000s. This peak  
418 is likely related to the maximum ammonium concentration shown in Figure 6. Moreover,  
419 flow/chlorophyll relationships have generally been constant throughout the period of record  
420 such that a change in flow has not been related to a change in phytoplankton production.  
421 This suggests that nutrient loads that contribute to production at P8 are primarily from  
422 point sources at WWTP outflows as a change in flow does not affect the load output. But  
423 what are watershed loads?

424 What do nitrogen trends mean? Have to interpret relative to trends in other variables.  
425 A decrease in nitrogen or constant nitrogen does not mean nitrogen inputs have stayed the  
426 same, they might actually be increasing if nitrogen. A change in chlorophyll relative to  
427 change in nitrogen could be informative, and even moreso, a change in silica relative to  
428 change in chlorophyll suggests diatom biomass has changed. However, there are mismatches  
429 in these trends that suggest other processes are at play, e.g., residence times and flow in-  
430 puts, etc. Trends in Suisun relative to trends in Delta provide an example, e.g., Suisun is  
431 decrease in chlorophyll, increase in silica, increase in nitrogen, delta is decrease in silica, in-  
432 crease/decrease in DIN (depending on time period/season), decrease in chlorophyll, what's

433 going on? See Senn slide 14 (from burial?). The WRTDS model lets us at least address  
434 trends in the context of season, time, and flow. This allows for more improved interpretation  
435 relative to observing raw data. Also explain more information by looking at ammonium,  
436 nitrate/nitrite, relative to DIN. What about other variables (light level as suspended par-  
437 ticulate matter, temperature)?

## 438 4 References

### 439 References

- 440 (1) O'Neill, R. V.; Johnson, A. R.; King, A. W. A hierarchical framework for the analysis  
441 of scale. *Landscape Ecology* **1989**, *3*, 193–205.
- 442 (2) Levin, S. A. The problem of pattern and scale in ecology. *Ecology* **1992**, *73*, 1943–1967.
- 443 (3) Bhangu, I.; Whitfield, P. H. Seasonal and long-term variations in water quality of the  
444 Skeena River at Usk, British Columbia. *Water Research* **1997**, *31*, 2187–2194.
- 445 (4) Champely, S.; Doledec, S. How to separate long-term trends from periodic variation in  
446 water quality monitoring. *Water Research* **1997**, *31*, 2849–2857.
- 447 (5) Chang, H. Spatial analysis of water quality trends in the Han River basin, South Korea.  
448 *Water Research* **2008**, *42*, 3285–3304.
- 449 (6) Halliday, S. J.; Wade, A. J.; Skeffington, R. A.; Neal, C.; Reynolds, B.; Rowland, P.;  
450 Neal, M.; Norris, D. An analysis of long-term trends, seasonality and short-term dy-  
451 namics in water quality data from Plynlimon, Wales. *Science of the Total Environment*  
452 **2012**, *434*, 186–200.
- 453 (7) Cloern, J. E. Phytoplankton bloom dynamics in coastal ecosystems: A review with  
454 some general lessons from sustained investigation of San Francisco Bay, California.  
455 *Review of Geophysics* **1996**, *34*, 127–168.
- 456 (8) Cloern, J. E.; Jassby, A. D. Patterns and scales of phytoplankton variability in  
457 estuarine-coastal ecosystems. *Estuaries and Coasts* **2010**, *33*, 230–241.
- 458 (9) Sakamoto, M.; Tanaka, T. Phosphorus dynamics associated with phytoplankton blooms  
459 in eutrophic Mikawa Bay, Japan. *Marine Biology* **1989**, *101*, 265–271.
- 460 (10) Schultz, P.; Urban, N. R. Effects of bacterial dynamics on organic matter decomposition  
461 and nutrient release from sediments: A modeling study. *Ecological Modelling* **2008**, *210*,  
462 1–14.

- 463 (11) Harding, L. W.; Gallegos, C. L.; Perry, E. S.; Miller, W. D.; Adolf, J. E.; Mal-  
464 lonee, M. E.; Paerl, H. W. Long-term trends of nutrients and phytoplankton in Chesa-  
465 peake Bay. *Estuaries and Coasts* **2016**, *39*, 664–681.
- 466 (12) Hirsch, R. M.; Alexander, R. B.; Smith, R. A. Selection of methods for the detection  
467 and estimation of trends in water quality. *Water Resources Research* **1991**, *27*, 803–813.
- 468 (13) Esterby, S. R. Review of methods for the detection and estimation of trends with  
469 emphasis on water quality applications. *Hydrological Processes* **1996**, *10*, 127–149.
- 470 (14) Bowes, M. J.; Smith, J. T.; Neal, C. The value of high resolution nutrient monitoring:  
471 a case study of the River Frome, Dorset, UK. *Journal of Hydrology* **2009**, *378*, 82–96.
- 472 (15) Hirsch, R. M.; Moyer, D. L.; Archfield, S. A. Weighted regressions on time, discharge,  
473 and season (WRTDS), with an application to Chesapeake Bay river inputs. *Journal of*  
474 *the American Water Resources Association* **2010**, *46*, 857–880.
- 475 (16) Sprague, L. A.; Hirsch, R. M.; Aulenbach, B. T. Nitrate in the Mississippi River and  
476 its tributaries, 1980 to 2008: Are we making progress? *Environmental Science and*  
477 *Technology* **2011**, *45*, 7209–7216.
- 478 (17) Medalie, L.; Hirsch, R. M.; Archfield, S. A. Use of flow-normalization to evaluate nutri-  
479 ent concentration and flux changes in Lake Champlain tributaries, 1990–2009. *Journal*  
480 *of Great Lakes Research* **2012**, *38*, 58–67.
- 481 (18) Hirsch, R. M.; De Cicco, L. *User guide to Exploration and Graphics for RivEr Trends*  
482 (*EGRET*) and *dataRetrieval: R packages for hydrologic data*; 2014; p 94, [http://](http://pubs.usgs.gov/tm/04/a10/)  
483 [pubs.usgs.gov/tm/04/a10/](http://pubs.usgs.gov/tm/04/a10/).
- 484 (19) Zhang, Q.; Harman, C. J.; Ball, W. P. An improved method for interpretation of riverine  
485 concentration-discharge relationships indicates long-term shifts in reservoir sediment  
486 trapping. *Geophysical Research Letters* **2016**, *43*, 215–224.
- 487 (20) Beck, M. W.; Hagy III, J. D. Adaptation of a weighted regression approach to evaluate  
488 water quality trends in an estuary. *Environmental Modelling and Assessment* **2015**, *20*,  
489 637–655.
- 490 (21) Beck, M. W.; Murphy, R. R. Numerical and qualitative contrasts of two statistical mod-  
491 els for water quality change in tidal waters. *Journal of the American Water Resources*  
492 *Association* In press,
- 493 (22) Beck, M. W.; Hagy III, J. D.; Murrell, M. C. Improving estimates of ecosystem  
494 metabolism by reducing effects of tidal advection on dissolved oxygen time series. *Lim-  
495 nology and Oceanography: Methods* **2015**, *13*, 731–745.
- 496 (23) Cloern, J. E. In *Ecosystems of California: A Source Book*; Mooney, H., Zavaleta, E.,  
497 Eds.; University of California Press: California, 2015; pp 359–387.

- 498 (24) Cloern, J. E.; Jassby, A. D. Drivers of change in estuarine-coastal ecosystems: Discov-  
499 eries from four decades of study in San Francisco Bay. *Reviews of Geophysics* **2012**,  
500 *50*, 1–33.
- 501 (25) Jassby, A. D.; Cloern, J. E. Organic matter sources and rehabilitations of the  
502 Sacramento-San Joaquin Delta (California, USA). **2000**,
- 503 (26) Jassby, A. D.; Cloern, J. E.; Cole, B. E. Annual primary production: Patterns and  
504 mechanisms of change in a nutrient-rich tidal ecosystem. *Limnology and Oceanography*  
505 **2002**, *47*, 698–712.
- 506 (27) Jassby, A. D. Phytoplankton in the Upper San Francisco Estuary: Recent biomass  
507 trends, their causes, and their trophic significance. *San Francisco Estuary and Water-  
508 shed Science* **2008**, *6*, 1–24.
- 509 (28) Jabusch, T.; Bresnahan, P.; Trowbridge, P.; Novick, E.; Wong, A.; Salomon, M.;  
510 Senn, D. *Summary and evaluation of Delta subregions for nutrient monitoring and  
511 assessment*; 2016.
- 512 (29) Novick, E.; Holleman, R.; Jabusch, T.; Sun, J.; Trowbridge, P.; Senn, D.; Guerin, M.;  
513 Kendall, C.; Young, M.; Peek, S. *Characterizing and quantifying nutrient sources, sinks  
514 and transformations in the Delta: synthesis, modeling, and recommendations for mon-  
515 itoring*; 2015.
- 516 (30) Cloern, J. E.; Jassby, A. D.; Thompson, J. K.; Hieb, K. A. A cold phase of the East  
517 Pacific triggers new phytoplankton blooms in San Francisco Bay. *Proceedings of the  
518 National Academy of Sciences of the United States of America* **2007**, *104*, 18561–18565.
- 519 (31) Kemp, W. M. et al. Eutrophication of Chesapeake Bay: historical trends and ecological  
520 interactions. *Marine Ecology Progress Series* **2005**, *303*, 1–29.
- 521 (32) Kimmerer, W. J.; Parker, A. E.; Lidstrom, U. E.; Carpenter, E. J. Short-term and in-  
522 terannual variability in primary production in the low-salinity zone of the San Francisco  
523 Estuary. *Estuaries and Coasts* **2012**, *35*, 913–929.
- 524 (33) Thompson, J. K.; Koseff, J. R.; Monismith, S. G.; Lucas, L. V. Shallow water processes  
525 govern system-wide phytoplankton bloom dynamics: A field study. *Journal of Marine  
526 Systems* **2008**, *74*, 153–166.
- 527 (34) Crauder, J. S.; Thompson, J. K.; Parchaso, F.; Anduaga, R. I.; Pearson, S. A.;  
528 Gehrtz, K.; Fuller, H.; Wells, E. *Bivalve effects on the food web supporting delta smelt  
529 - A long-term study of bivalve recruitment, biomass, and grazing rate patterns with  
530 varying freshwater outflow*; 2016.
- 531 (35) Sutula, M.; Kudela, R.; III, J. D. H.; Jr., L. W. H.; Senn, D.; Cloern, J. E.; Bricker, S.;  
532 Berg, G. M.; Beck, M. W. Novel analyses of long-term data provide a scientific basis  
533 for chlorophyll-a thresholds in San Francisco Bay. *Estuarine, Coastal and Shelf Science  
534 in review*,

- 535 (36) Lehman, P. W.; Boyer, G.; Hall, C.; Waller, S.; Gehrts, K. Distribution and toxicity  
536 of a new colonial *Microcystis aeruginosa* bloom in the San Francisco Bay Estuary,  
537 California. *Hydrobiologia* **2005**, *541*, 87–99.
- 538 (37) Lehman, P. W.; Teh, S. J.; Boyer, G. L.; Nobriga, M. L.; Bass, E.; Hogle, C. Initial  
539 impacts of *Microcystis aeruginosa* blooms on the aquatic food web in the San Francisco  
540 Estuary. *Hydrobiologia* **2010**, *637*, 229–248.
- 541 (38) Cohen, A. N.; Carlton, J. T. Accelerating invasion rate in a highly invaded estuary.  
542 *Science* **1998**, *279*, 555–558.
- 543 (39) Enright, C.; Culberson, S. D. Salinity trends, variability, and control in the northern  
544 reach of the San Francisco Estuary. *San Francisco Estuary & Watershed Science* **2009**,  
545 *7*, 1–28.
- 546 (40) Dugdale, R. C.; Wilkerson, F. P.; Hogue, V. E.; Marchi, A. The role of ammonium and  
547 nitrate in spring bloom development in San Francisco Bay. *Estuarine, Coastal, and*  
548 *Shelf Science* **2007**, *73*, 17–29.
- 549 (41) Parker, A. E.; Hogue, V. E.; Wilkerson, F. P.; Dugdale, R. C. The effect of inorganic  
550 nitrogen speciation on primary production in the San Francisco Estuary. *Estuarine,*  
551 *Coastal, and Shelf Science* **2012**, *104*, 91–101.
- 552 (42) Glibert, P. M.; Dugdale, R. C.; Wilkerson, F.; Parker, A. E.; Alexander, J.; Antell, E.;  
553 Blaser, S.; Johnson, A.; Lee, J.; Lee, T.; Murasko, S.; Strong, S. Major - but rare -  
554 spring blooms in San Francisco Bay Delta, California, a result of long-term drought,  
555 increased residence time, and altered nutrient loads and forms. *Journal of Experimental*  
556 *Marine Biology and Ecology* **2014**, *460*, 8–18.
- 557 (43) IEP, IEP Bay-Delta Monitoring and Analysis Section, Discrete Water Quality Meta-  
558 data. 2013; <http://water.ca.gov/bdma/meta/discrete.cfm>.
- 559 (44) IEP, Dayflow: An estimate of daily average Delta outflow. Interagency Ecological Pro-  
560 gram for the San Francisco Estuary. 2016; <http://www.water.ca.gov/dayflow/>.
- 561 (45) Moyer, D. L.; Hirsch, R. M.; Hyer, K. E. *Comparison of two regression-based approaches*  
562 *for determining nutrient and sediment fluxes and trends in the Chesapeake Bay Water-*  
563 *shed*; 2012; p 118.
- 564 (46) Tobin, J. Estimation of relationships for limited dependent variables. *Econometrica*  
565 *1958*, *26*, 24–36.
- 566 (47) Beck, M. W. WRTDStidal: Weighted Regression for Water Quality Evaluation in Tidal  
567 Waters. 2016; R package version 1.0.2.
- 568 (48) RDCT (R Development Core Team), R: A language and environment for statistical  
569 computing, v3.3.1. R Foundation for Statistical Computing, Vienna, Austria. 2016;  
570 <http://www.R-project.org>.

- 571 (49) Hirsch, R. M.; Slack, J. R.; Smith, R. A. Techniques of trend analysis for monthly water  
572 quality data. *Water Resources Research* **1982**, *18*, 107–121.
- 573 (50) Millard, S. P. *EnvStats: An R Package for Environmental Statistics*; Springer: New  
574 York, 2013.
- 575 (51) Cornwell, J. C.; Glibert, P. M.; Owens, M. S. Nutrient fluxes from sediments in the San  
576 Francisco Bay Delta. *Estuaries and Coasts* **2014**, *37*, 1120–1133.
- 577 (52) Carlton, J. T.; Thompson, J. K.; Schemel, L. E.; Nichols, F. H. Remarkable invasion  
578 of San Francisco Bay (California, USA) by the Asian clam *Potamocorbula amurensis*.  
579 I. Introduction and dispersal. *Marine Ecology Progress Series* **1990**, *66*, 81–94.
- 580 (53) Nichols, F. H.; Thompson, J. K.; Schemel, L. E. Remarkable invasion of San Francisco  
581 Bay (California, USA) by the Asian clam *Potamocorbula amurensis*. II. Displacement  
582 of a former community. *Marine Ecology Progress Series* **1990**, *66*, 95–101.
- 583 (54) Werner, I.; Hollibaugh, J. T. *Potamocorbula amurensis* - comparison of clearance rates  
584 and assimilation efficiencies for phytoplankton and bacterioplankton. *Limnology and  
585 Oceanography* **1993**, *38*, 949–964.
- 586 (55) Feyrer, F.; Herbold, B.; Matern, S. A.; Moyle, P. B. Dietary shifts in a stressed fish  
587 assemblage: Consequences of a bivalve invasion in the San Francisco Estuary. *Environmental  
588 Biology of Fishes* **2003**, *67*, 277–288.
- 589 (56) Mac Nally, R.; Thompson, J. R.; Kimmerer, W. J.; Feyrer, F.; Newman, K. B.; Sih, A.;  
590 Bennett, W. A.; Brown, L.; Fleishman, E.; Culberson, S. D.; Castillo, G. Analysis of  
591 pelagic species decline in the upper San Francisco Estuary using multivariate autore-  
592 gressive modeling (MAR). *Ecological Applications* **2010**, *20*, 1417–1430.
- 593 (57) Parchaso, F.; Thompson, J. K. Influence of hydrologic processes on reproduction of the  
594 introduced bivalve *Potamocorbula amurensis* in northern San Francisco Bay, California.  
595 *Pacific Science* **2002**, *56*, 329–345.
- 596 (58) Alpine, A. E.; Cloern, J. E. Trophic interactions and direct physical effects control  
597 phytoplankton biomass and production in an estuary. *Limnology and Oceanography*  
598 **1992**, *37*, 946–955.

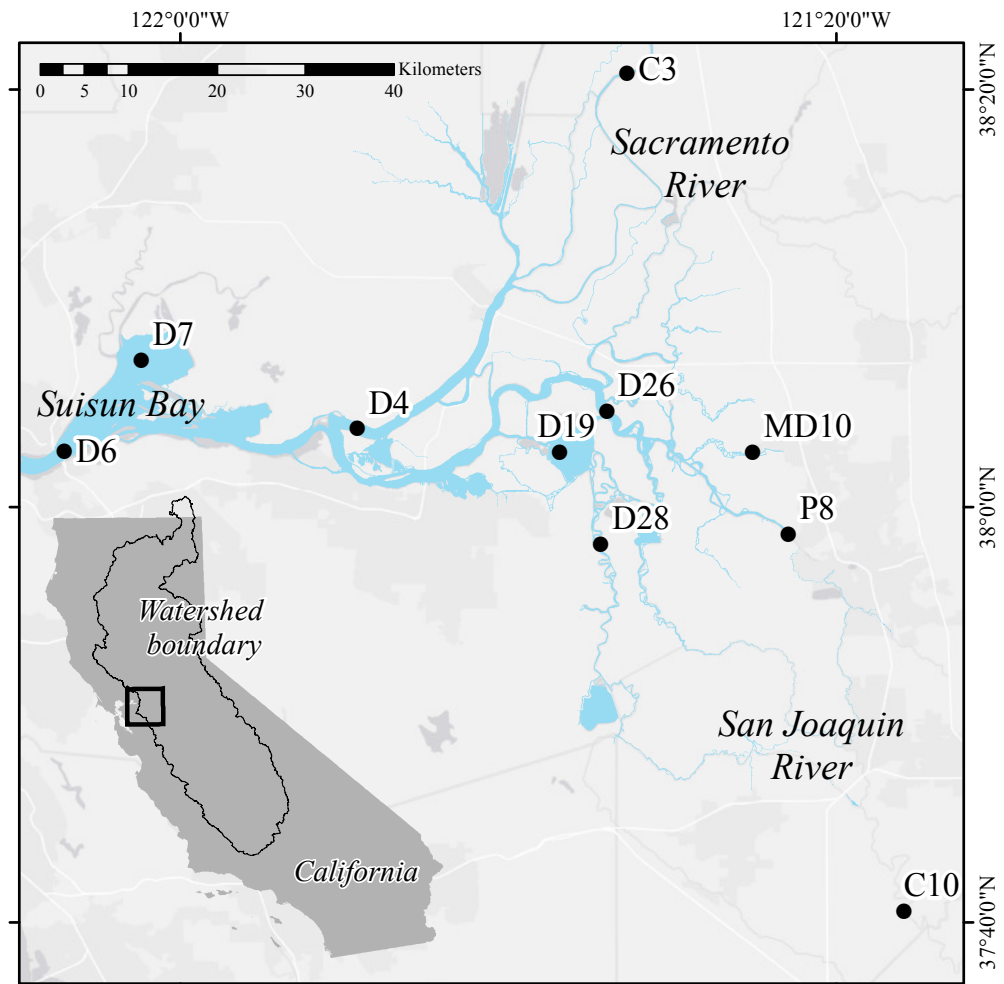


Figure 1: The San Francisco Estuary Delta and monitoring stations used for analysis. The Delta drains the combined watershed from the Sacramento and San Joaquin rivers (bottom left). All data were obtained from the Interagency Ecological Program website (<http://water.ca.gov/bdma/meta/Discrete/data.cfm>).<sup>43</sup>

{fig:delt\_m}

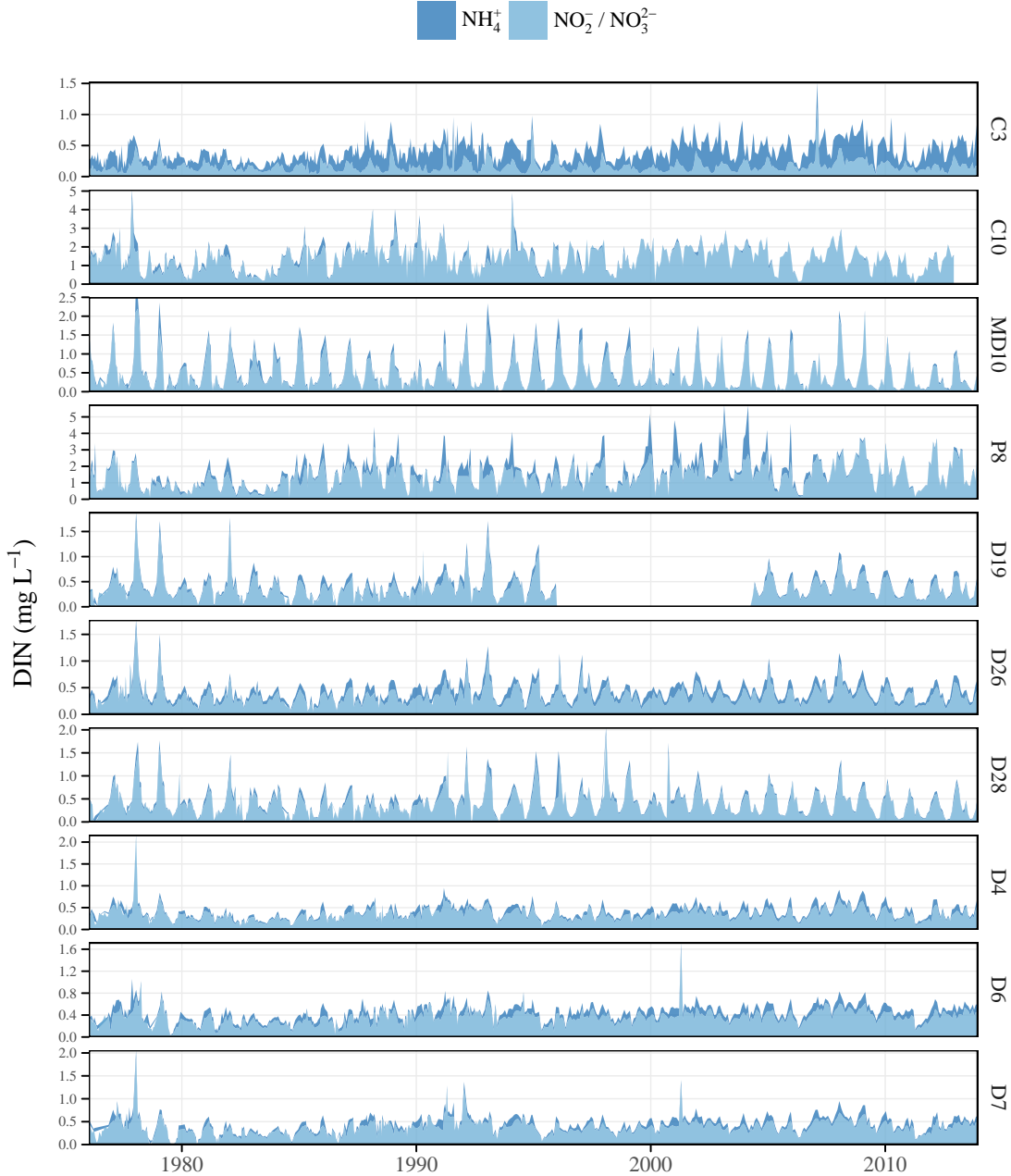


Figure 2: Observed DIN ( $\text{NH}_4^+ + \text{NO}_2^-/\text{NO}_3^{2-}$ ) from ten stations in the upper SFE Delta. Data were collected monthly and evaluated with WRTDS models from 1976 to 2013. Note different y-axis scales. See Figure 1 for station locations.

{fig:obsdat}

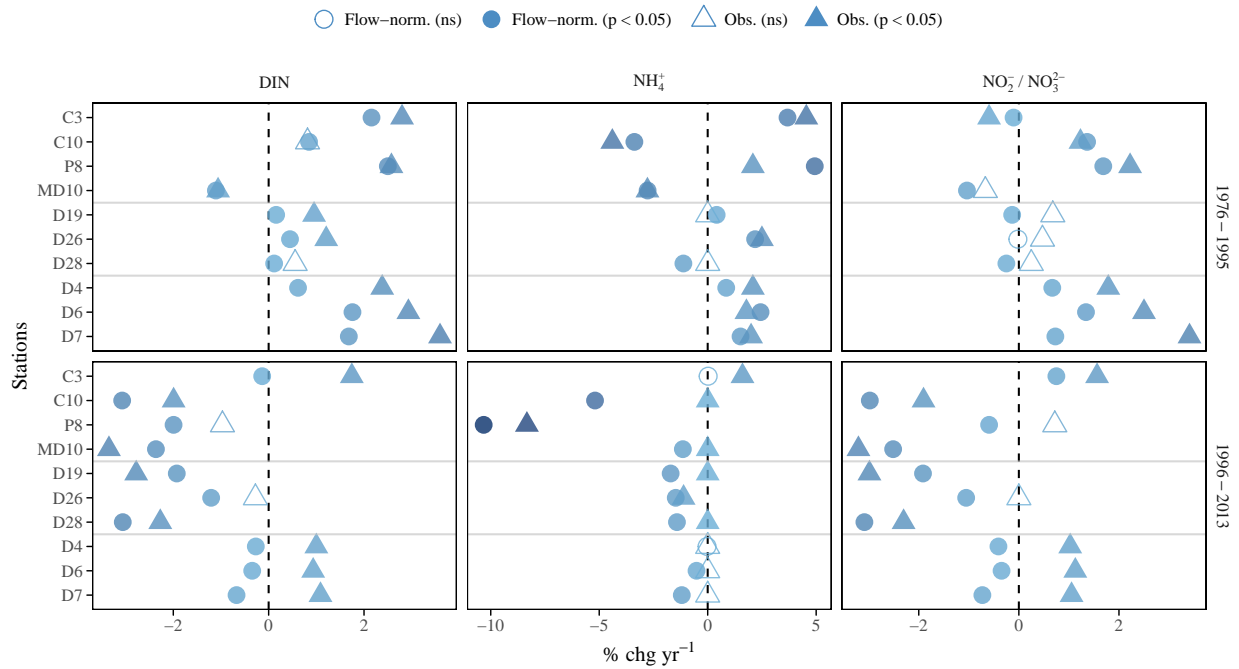


Figure 3: Results from seasonal Kendall tests on observed data (triangles) and flow-normalized predictions (circles) from WRTDS for nitrogen analytes. Results are shown as the percent change per year as the estimated Theil-Sen slope divided by the median for a given aggregation period (significance evaluated at  $\alpha = 0.05$ , based on  $\tau$ ). Trends are shown separately for different annual groupings. See Figures S1 and S2 for seasonal groupings.

{fig:trndcc}

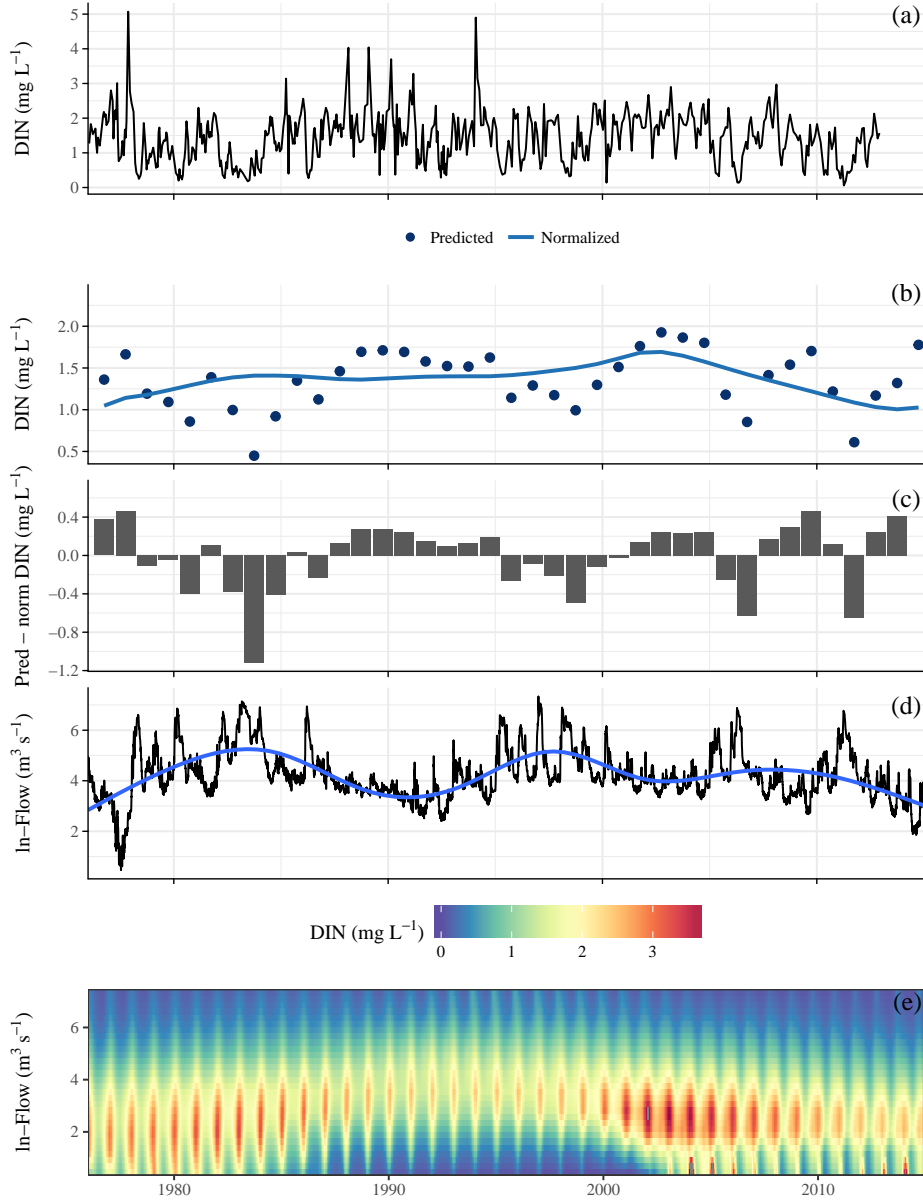


Figure 4: Time series of DIN and flow at station C10. Subfigure (a) shows the observed DIN time series and subfigure (b) shows the annual (water year starting in October) predictions from WRTDS for the conditional mean response. The points in subfigure (b) are predictions of observed DIN and the lines are flow-normalized predictions. Subfigure (c) shows the difference between the model predictions and flow-normalized predictions. Subfigure (d) shows the flow time series of the San Joaquin River with a locally-estimated (loess) smooth to emphasize the long-term trend. Subfigure (e) shows the modelled relationships between DIN, flow, and time.

{fig:dinc10}

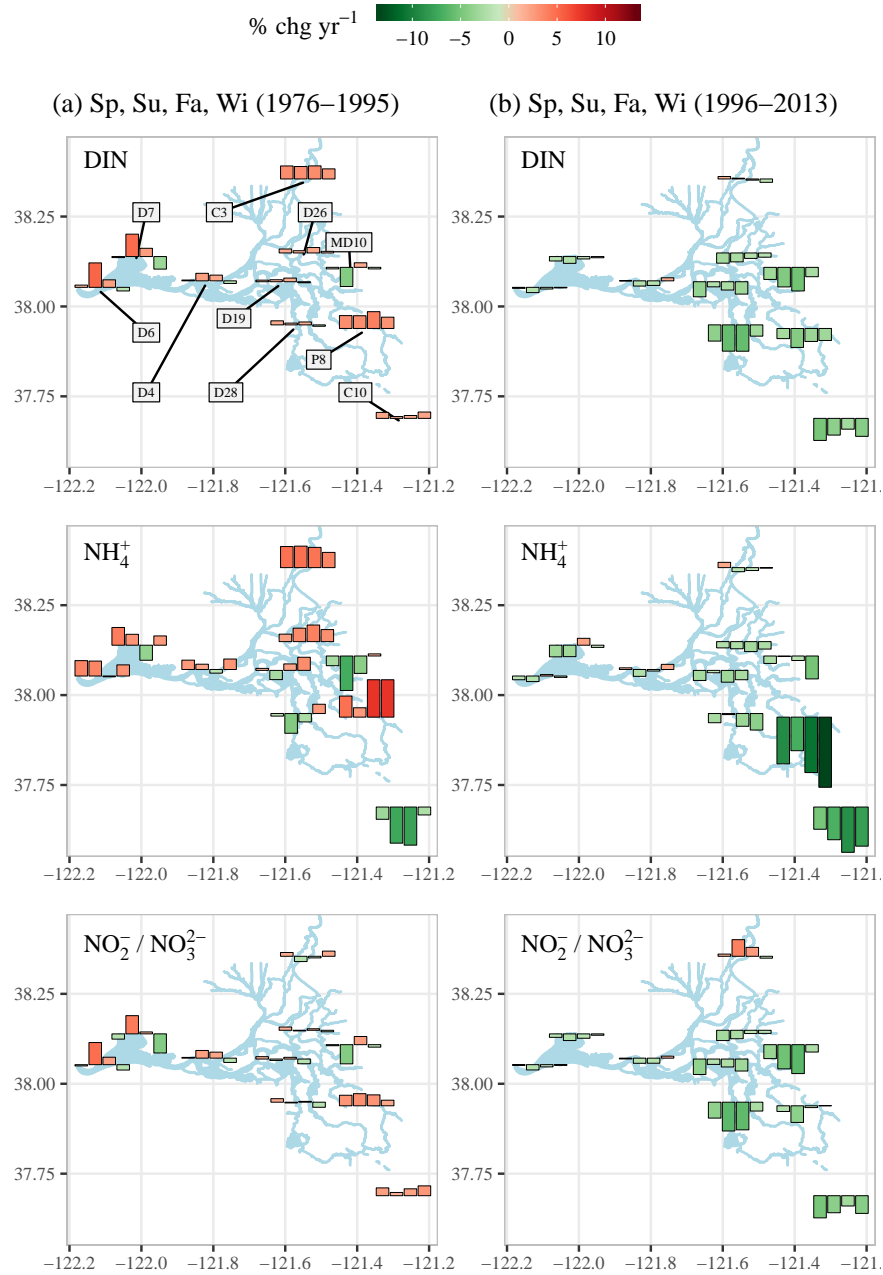


Figure 5: Percent change per year in nitrogen analytes for aggregations by seasons from (a) 1976-1995 and (b) 1996-2013. Changes are based on seasonal Kendall tests of flow-normalized results within each time period. Station names are shown in the top left panel. Station locations have been jittered to reduce overlap. Months for each season are Spring: MAM, Summer: JJA, Fall: SON, Winter: DJF.

{fig:trndma}

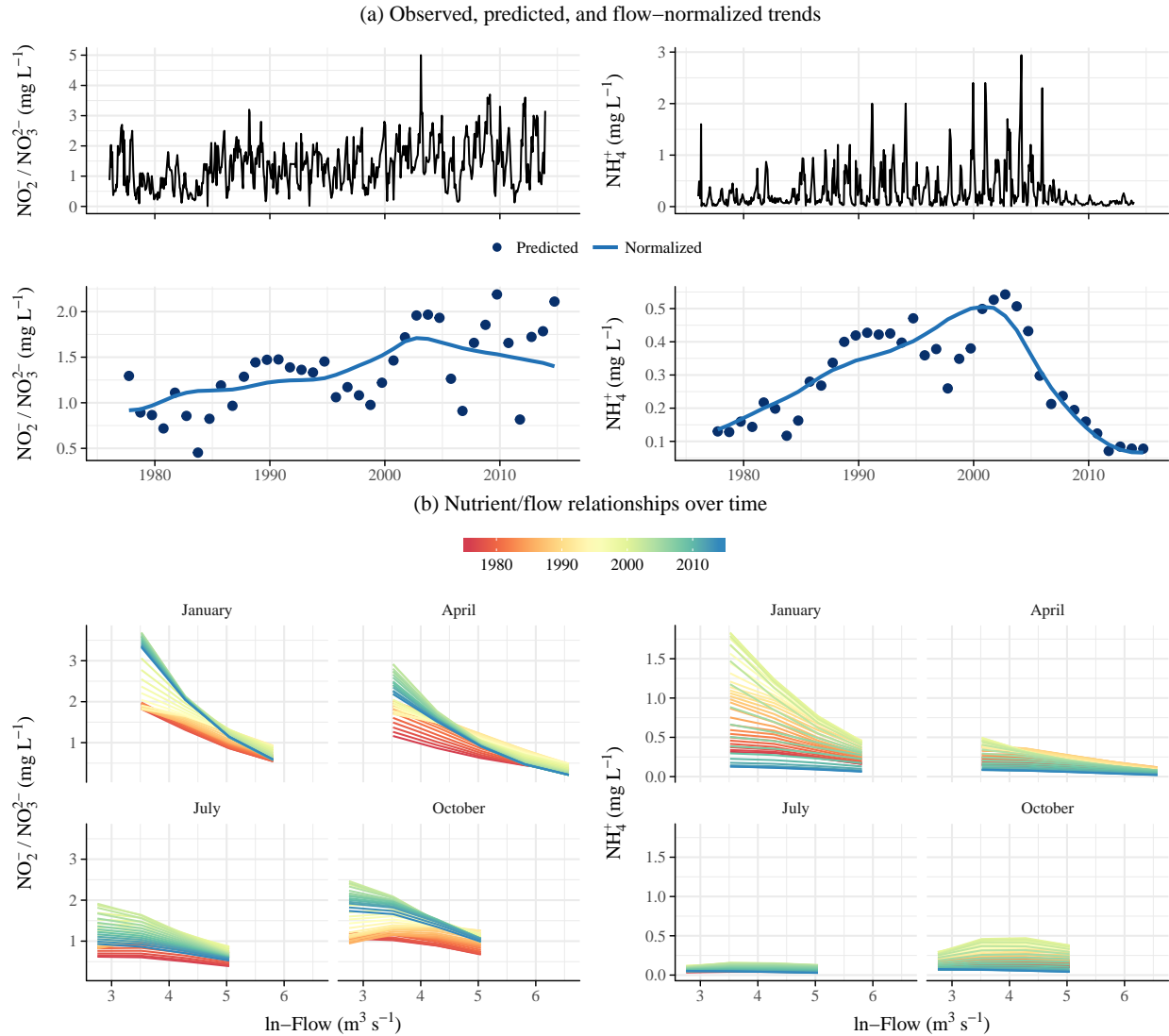


Figure 6: Nitrogen trends at P8 as observed (a, top), predicted and flow-normalized estimates from WRTDS (a, bottom), and relationships with flow over time (b). Nitrite/nitrate trends are on the left and ammonium trends are on the right. Wastewater treatment plant upgrades at the City of Stockton (San Joaquin County) were completed in 2006 (Figure S3), coincident with a dramatic decrease in ammonium at P8.

{fig:p8trnd}

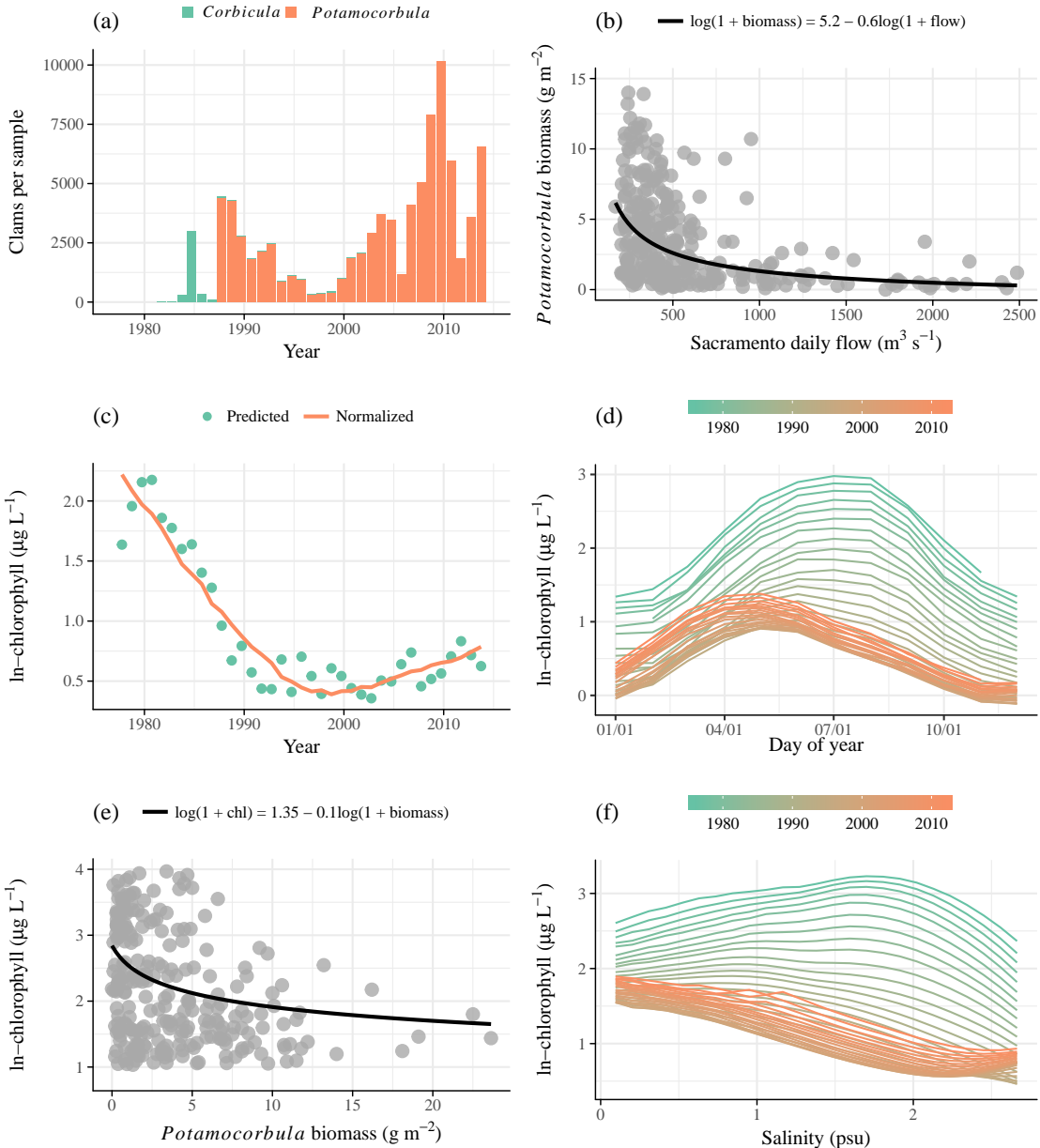


Figure 7: Trends in clam abundance and chl-*a* concentration from 1976 to 2013 at station D7 in Suisun Bay. Invasion by *Potamocorbula amurensis* clams in the late 1980s and displacement of *Corbicula fluminea* was shown by changes in clam density (a, annual means), with biomass linked to salinity (b). A coincident decrease in chl-*a* concentration was also observed by changes in annual (c) and seasonal trends(d). A significant ( $p < 0.001$ ) relationship between clam biomass and chl-*a* concentration is shown in subfigure (e). Flow relationships with chl-*a* concentration have also changed over time (f, observations from June).

{fig:clmchl}

Table 1: Summaries of flow-normalized trends in nitrogen analytes for all stations and annual aggregations. Summaries are medians ( $\text{mg L}^{-1}$ ) and percent change per year in parentheses (increasing in bold-italic). Changes and significance estimates are based on seasonal Kendall tests of flow-normalized results within each time period. See Figure 5 for a summary of spatial trends.

{tab:trndsa}

Analyte/Station	Annual	
	1976-1995	1996-2013
<b>DIN</b>		
C10	1.3 ( <b>0.8</b> )**	1.4 (-3.1)**
C3	0.3 ( <b>2.2</b> )**	0.5 (-0.1)**
D19	0.4 ( <b>0.2</b> )**	0.4 (-1.9)**
D26	0.4 ( <b>0.4</b> )**	0.5 (-1.2)**
D28	0.4 ( <b>0.1</b> )**	0.4 (-3.1)**
D4	0.3 ( <b>0.6</b> )**	0.4 (-0.3)**
D6	0.4 ( <b>1.8</b> )**	0.5 (-0.3)**
D7	0.4 ( <b>1.7</b> )**	0.5 (-0.7)**
MD10	0.4 (-1.1)**	0.3 (-2.4)**
P8	1.3 ( <b>2.5</b> )**	1.7 (-2)**
<b>NH<sub>4</sub><sup>+</sup></b>		
C10	0.1 (-3.4)**	0 (-5.2)**
C3	0.2 ( <b>3.7</b> )**	0.3 ( <b>0</b> )
D19	0 ( <b>0.4</b> )**	0 (-1.7)**
D26	0.1 ( <b>2.2</b> )**	0.1 (-1.5)**
D28	0 (-1.1)**	0 (-1.4)**
D4	0 ( <b>0.9</b> )**	0.1 ( <b>0</b> )
D6	0.1 ( <b>2.4</b> )**	0.1 (-0.5)**
D7	0.1 ( <b>1.5</b> )**	0.1 (-1.2)**
MD10	0.1 (-2.8)**	0 (-1.1)**
P8	0.2 ( <b>4.9</b> )**	0.1 (-10.3)**
<b>NO<sub>2</sub><sup>-</sup>/NO<sub>3</sub><sup>2-</sup></b>		
C10	1.2 ( <b>1.4</b> )**	1.4 (-3)**
C3	0.1 (-0.1)**	0.2 ( <b>0.7</b> )**
D19	0.4 (-0.1)**	0.4 (-1.9)**
D26	0.3 ( <b>0</b> )	0.4 (-1.1)**
D28	0.4 (-0.2)**	0.4 (-3.1)**
D4	0.3 ( <b>0.7</b> )**	0.3 (-0.4)**
D6	0.3 ( <b>1.3</b> )**	0.4 (-0.3)**
D7	0.4 ( <b>0.7</b> )**	0.4 (-0.7)**
MD10	0.4 (-1)**	0.3 (-2.5)**
P8	1.2 ( <b>1.7</b> )**	1.5 (-0.6)**

\* $p < 0.05$ ; \*\* $p < 0.005$

Table 2: Summaries of flow-normalized trends in nitrogen analytes for all stations and seasonal aggregations from 1976-1995. Summaries are medians ( $\text{mg L}^{-1}$ ) and percent change per year in parentheses (increasing in bold-italic). Changes and significance estimates are based on seasonal Kendall tests of flow-normalized results within each time period. See Figure 5 for a summary of spatial trends. Months for each season are Spring: MAM, Summer: JJA, Fall: SON, Winter: DJF.

{tab:trndsb}

Analyte/Station	Seasonal, 1976-1995			
	Spring	Summer	Fall	Winter
<b>DIN</b>				
C10	1.2 ( <b>1.1</b> )**	1.2 ( <b>0.3</b> )	1.3 ( <b>0.5</b> )**	1.7 ( <b>1.2</b> )**
C3	0.3 ( <b>2.4</b> )**	0.3 ( <b>2.3</b> )**	0.4 ( <b>2.4</b> )**	0.4 ( <b>1.9</b> )**
D19	0.5 ( <b>0.3</b> )	0.2 ( <b>0.4</b> )	0.3 ( <b>0.7</b> )**	0.7 (-0.2)
D26	0.4 ( <b>0.7</b> )**	0.3 ( <b>0.4</b> )*	0.4 ( <b>1</b> )**	0.6 ( <b>0.3</b> )
D28	0.5 ( <b>0.8</b> )*	0.2 ( <b>0.3</b> )	0.3 ( <b>0.5</b> )*	0.8 (-0.3)
D4	0.4 ( <b>0.2</b> )	0.3 ( <b>1.4</b> )**	0.3 ( <b>1.1</b> )**	0.5 (-0.5)
D6	0.4 ( <b>0.4</b> )	0.3 ( <b>4.6</b> )**	0.4 ( <b>1.4</b> )**	0.5 (-0.7)*
D7	0.4 (-0.2)	0.3 ( <b>4.2</b> )**	0.4 ( <b>1.5</b> )**	0.6 (-2.4)**
MD10	0.6 (-0.3)	0.2 (-3.6)**	0.3 ( <b>0.8</b> )**	1.3 (-0.3)*
P8	1.3 ( <b>2.4</b> )**	0.9 ( <b>2.4</b> )**	1.3 ( <b>3.1</b> )**	1.9 ( <b>2.1</b> )**
<b>NH<sub>4</sub><sup>+</sup></b>				
C10	0.1 (-2.3)**	0 (-6.8)**	0.1 (-7.1)**	0.3 (-1.5)**
C3	0.2 ( <b>3.9</b> )**	0.2 ( <b>4</b> )**	0.3 ( <b>3.8</b> )**	0.2 ( <b>2.9</b> )**
D19	0.1 ( <b>0.4</b> )*	0 (-1.7)**	0 ( <b>1.2</b> )**	0.1 ( <b>2.5</b> )**
D26	0.1 ( <b>1.4</b> )**	0.1 ( <b>2.5</b> )**	0.1 ( <b>3.1</b> )**	0.1 ( <b>2.3</b> )**
D28	0.1 (-0.5)	0 (-3.7)**	0 (-1.6)**	0.1 ( <b>1.7</b> )**
D4	0.1 ( <b>1.7</b> )**	0 ( <b>1</b> )**	0 (-0.7)	0.1 ( <b>2</b> )**
D6	0.1 ( <b>2.9</b> )**	0.1 ( <b>2.8</b> )**	0.1 (-0.1)	0.1 ( <b>2.1</b> )**
D7	0.1 ( <b>3.3</b> )**	0 ( <b>2</b> )**	0.1 (-2.8)**	0.1 ( <b>1.7</b> )**
MD10	0.1 (-1.8)**	0 (-6.5)**	0 (-3.3)**	0.2 ( <b>0.4</b> )
P8	0.2 ( <b>3.9</b> )**	0.1 ( <b>1.8</b> )**	0.2 ( <b>7</b> )**	0.6 ( <b>7</b> )**
<b>NO<sub>2</sub><sup>-</sup>/NO<sub>3</sub><sup>2-</sup></b>				
C10	1.1 ( <b>1.5</b> )**	1.2 ( <b>0.6</b> )**	1.2 ( <b>1.3</b> )**	1.5 ( <b>1.8</b> )**
C3	0.2 ( <b>0.7</b> )**	0.1 (-1)**	0.1 (-0.3)	0.2 ( <b>1</b> )**
D19	0.4 ( <b>0.4</b> )	0.2 (-0.3)	0.3 ( <b>0.3</b> )	0.6 (-0.9)*
D26	0.4 ( <b>0.6</b> )*	0.2 (-0.1)	0.3 ( <b>0.3</b> )*	0.5 (-0.3)
D28	0.5 ( <b>0.7</b> )*	0.2 (-0.1)	0.3 ( <b>0.2</b> )	0.7 (-1)**
D4	0.3 ( <b>0.1</b> )	0.3 ( <b>1.4</b> )**	0.3 ( <b>1.1</b> )**	0.4 (-0.8)*
D6	0.4 (-0.2)	0.3 ( <b>4.1</b> )**	0.3 ( <b>1.4</b> )**	0.4 (-1)**
D7	0.4 (-1)*	0.3 ( <b>3.4</b> )**	0.4 ( <b>0.4</b> )	0.4 (-3.6)**
MD10	0.5 (-0.2)	0.2 (-3.6)**	0.2 ( <b>1.5</b> )**	1.2 (-0.5)*
P8	1.2 ( <b>2</b> )**	0.9 ( <b>2.3</b> )**	1.1 ( <b>2</b> )**	1.4 ( <b>1</b> )**

\* $p < 0.05$ ; \*\* $p < 0.005$

Table 3: Summaries of flow-normalized trends in nitrogen analytes for all stations and seasonal aggregations from 1996-2013. Summaries are medians ( $\text{mg L}^{-1}$ ) and percent change per year in parentheses (increasing in bold-italic). Changes and significance estimates are based on seasonal Kendall tests of flow-normalized results within each time period. See Figure 5 for a summary of spatial trends. Months for each season are Spring: MAM, Summer: JJA, Fall: SON, Winter: DJF.

{tab:trndsa}

Analyte/Station	Seasonal, 1996-2013			
	Spring	Summer	Fall	Winter
<b>DIN</b>				
C10	1.1 (-4.1)**	1.3 (-3.1)**	1.6 (-2)**	1.7 (-3.4)**
C3	0.5 ( <b>0.5</b> )	0.4 ( <b>0.1</b> )	0.6 (-0.2)	0.5 (-0.6)**
D19	0.5 (-2.8)**	0.2 (-1)*	0.3 (-1.6)**	0.7 (-2.3)**
D26	0.5 (-1.9)**	0.3 (-1.7)**	0.4 (-1)**	0.6 (-0.8)**
D28	0.5 (-3)**	0.2 (-4.9)**	0.2 (-4.9)**	0.7 (-2.1)**
D4	0.4 ( <b>0</b> )	0.4 (-1)**	0.4 (-0.9)**	0.5 ( <b>0.6</b> )**
D6	0.5 (-0.2)*	0.5 (-1)**	0.5 (-0.3)*	0.5 (-0.1)
D7	0.5 (-0.8)**	0.4 (-1.3)**	0.4 (-0.4)**	0.6 (-0.2)
MD10	0.4 (-2.3)**	0.2 (-3.7)**	0.2 (-4.4)**	1 (-1.8)**
P8	1.5 (-1.9)**	1.2 (-3.5)**	1.8 (-2.4)**	2.7 (-2.2)**
<b>NH<sub>4</sub><sup>+</sup></b>				
C10	0 (-4.2)**	0 (-6.1)**	0 (-8.5)**	0.1 (-7.3)**
C3	0.3 ( <b>1</b> )**	0.3 (-0.8)*	0.4 (-0.5)*	0.2 (-0.1)
D19	0 (-1.9)**	0 (-0.4)	0 (-2.2)**	0.1 (-1.8)**
D26	0.1 (-1.2)**	0.1 (-1.3)**	0.1 (-1.9)**	0.1 (-1.4)**
D28	0 (-1.7)**	0 (-0.2)	0 (-2.4)**	0.1 (-3.1)**
D4	0.1 ( <b>0.3</b> )	0 (-1.3)**	0.1 (-0.3)	0.1 ( <b>1</b> )**
D6	0.1 (-0.7)**	0.1 (-1)**	0.1 ( <b>0.3</b> )	0.1 (-0.3)**
D7	0.1 (-2.2)**	0 (-2.1)**	0.1 ( <b>1.3</b> )**	0.1 (-0.4)*
MD10	0 (-1.4)*	0 (-0.1)	0 (-0.8)**	0.1 (-4.3)**
P8	0.2 (-8.7)**	0.1 (-6.3)**	0.2 (-10.4)**	0.5 (-13.1)**
<b>NO<sub>2</sub><sup>-</sup>/NO<sub>3</sub><sup>2-</sup></b>				
C10	1.1 (-4.2)**	1.2 (-3.2)**	1.6 (-1.9)**	1.6 (-3.3)**
C3	0.2 ( <b>0.4</b> )	0.1 ( <b>3.1</b> )**	0.2 ( <b>1.7</b> )**	0.2 (-0.4)
D19	0.4 (-2.9)**	0.2 (-1)*	0.3 (-1.5)**	0.6 (-2.2)**
D26	0.4 (-1.9)**	0.2 (-1.6)**	0.3 (-0.6)*	0.5 (-0.6)**
D28	0.5 (-3)**	0.2 (-5.4)**	0.2 (-5.2)**	0.7 (-1.7)**
D4	0.3 (-0.1)	0.3 (-1)**	0.3 (-1)**	0.4 ( <b>0.4</b> )**
D6	0.4 (-0.1)	0.4 (-1)**	0.4 (-0.4)*	0.4 (-0.1)
D7	0.4 (-0.6)**	0.4 (-1.2)**	0.4 (-0.8)**	0.4 (-0.3)*
MD10	0.4 (-2.6)**	0.1 (-4.5)**	0.2 (-5.4)**	1 (-1.4)**
P8	1.3 (-1.1)**	1.1 (-3.1)**	1.6 (-0.3)*	2.2 ( <b>0</b> )

\* $p < 0.05$ ; \*\* $p < 0.005$

Table 4: Summaries of flow-normalized trends in nitrite/nitrate and ammonium ( $\text{mg L}^{-1}$ ) concentrations before and after WWTP upgrades upstream of station P8. Upgrades were completed in 2006 at the City of Stockton WWTP (San Joaquin County, Figure S3). Summaries are medians and percent change per year in parentheses (increasing in bold-italic). Changes and significance estimates are based on seasonal Kendall tests of flow-normalized results within each time period. Increasing values are in bold-italics. Months for each season are Spring: MAM, Summer: JJA, Fall: SON, Winter: DJF.

{tab:p8chg}

Period	$\text{NO}_2^-/\text{NO}_3^{2-}$		$\text{NH}_4^+$	
	Median	% change	Median	% change
<b>Annual</b>				
1976-2006	1.3	<b>2</b> **	0.2	<b>2.8</b> **
2007-2013	1.4	-1.9**	0.1	-16.6**
<b>Seasonal, pre</b>				
Spring	1.2	<b>1.6</b> **	0.2	<b>1.4</b> **
Summer	1	<b>2.4</b> **	0.1	<b>3.3</b> **
Fall	1.3	<b>2.2</b> **	0.2	<b>4.9</b> **
Winter	1.5	<b>2.1</b> **	0.7	<b>4.8</b> **
<b>Seasonal, post</b>				
Spring	1.3	-1.6**	0.1	-16.2**
Summer	0.9	-4.3**	0.1	-15.7**
Fall	1.5	-1.7**	0.1	-19.3**
Winter	2.2	-0.8**	0.2	-26.7**

\* $p < 0.05$ ; \*\* $p < 0.005$

Table 5: Summaries of flow-normalized trends in dissolved inorganic nitrogen ( $\text{mg L}^{-1}$ ), chlorophyll ( $\mu\text{g L}^{-1}$ ), and silicon dioxide ( $\text{mg L}^{-1}$ ) concentrations for different time periods at station D7. Summaries are medians and percent change per year in parentheses (increasing in bold-italic). Changes and significance estimates are based on seasonal Kendall tests of flow-normalized results within each time period. Increasing values are in bold-italics. Months for each season are Spring: MAM, Summer: JJA, Fall: SON, Winter: DJF.

{tab:d7ch}

Period	DIN		Chl-a		SiO <sub>2</sub>	
	Median	% change	Median	% change	Median	% change
<b>All</b>						
1976-2013	0.4	<b>0.6**</b>	3	-6.7**	12.7	<b>0.7**</b>
<b>Annual</b>						
1976-1985	0.4	-2.1**	8.8	-10.7**	10.2	-0.2
1986-1994	0.4	<b>3.6**</b>	2.6	-13.5**	11.9	<b>2.3**</b>
1995-2003	0.5	-0.1	1.8	<b>1.9**</b>	13.3	<b>0.7**</b>
2004-2013	0.5	-1.3**	2.1	<b>2.9**</b>	13.1	-0.3**
<b>Seasonal</b>						
Spring	0.5	-0.1	3.4	-1	14.7	<b>0.1**</b>
Summer	0.4	<b>1.5**</b>	3.4	-8.8**	12.2	<b>1.2**</b>
Fall	0.4	<b>0.6**</b>	1.7	-8.8**	12.1	<b>1**</b>
Winter	0.6	-0.2	1.4	-3.1**	14.5	<b>0.3**</b>

\* $p < 0.05$ ; \*\* $p < 0.005$

<sup>599</sup> **Supporting Information Available**

<sup>600</sup> The following files are available free of charge.

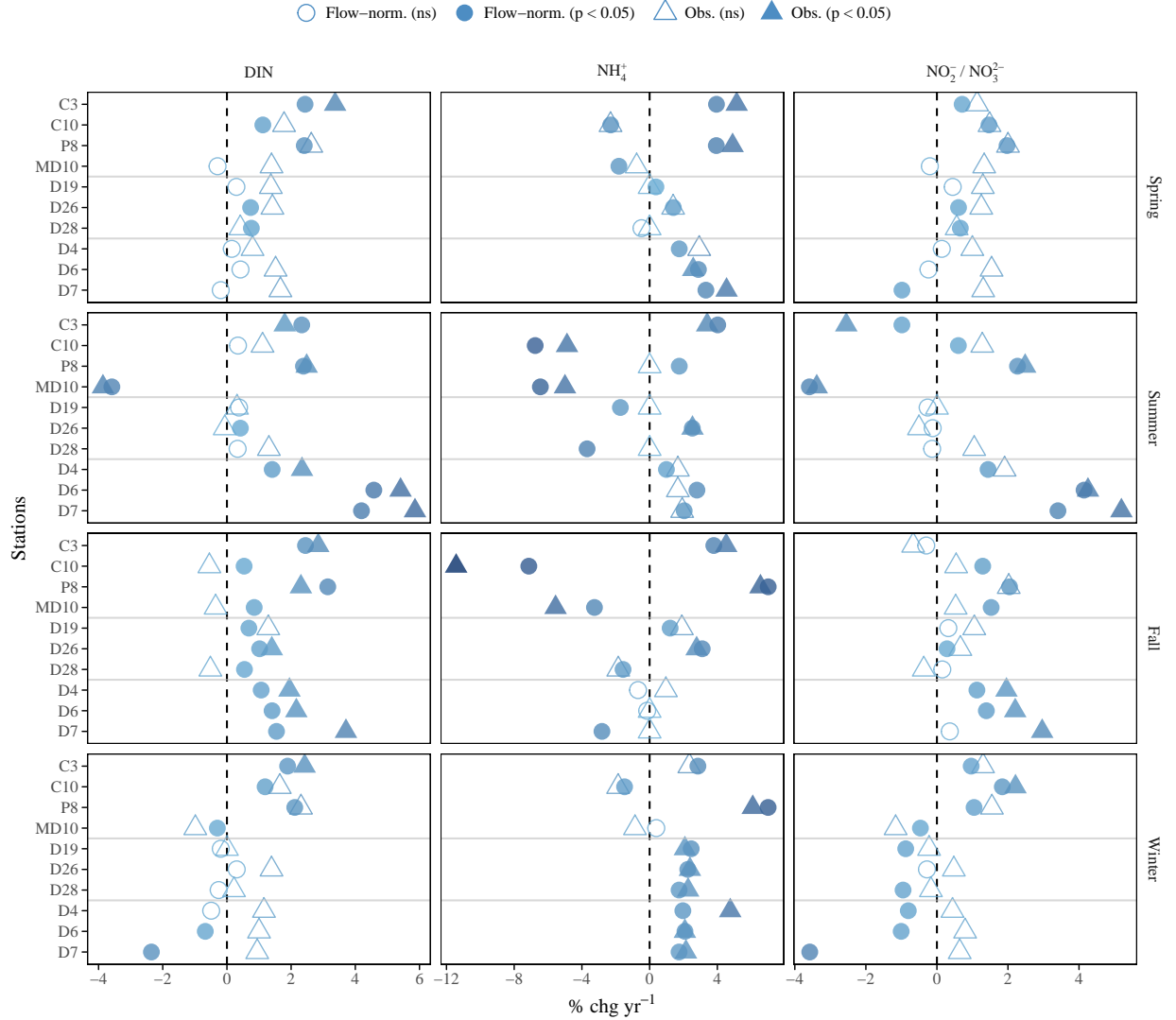


Figure S1: Results from seasonal Kendall tests on observed data (triangles) and flow-normalized predictions (circles) from WRTDS for nitrogen analytes. Results are shown as the percent change per year as the estimated Theil-Sen slope divided by the median for a given aggregation period (significance evaluated at  $\alpha = 0.05$ , based on  $\tau$ ). Trends are shown separately for different seasonal groupings from 1976-1995. Months for each season are Spring: MAM, Summer: JJA, Fall: SON, Winter: DJF. See Figure 3 for annual comparisons.

{fig:trndcc}

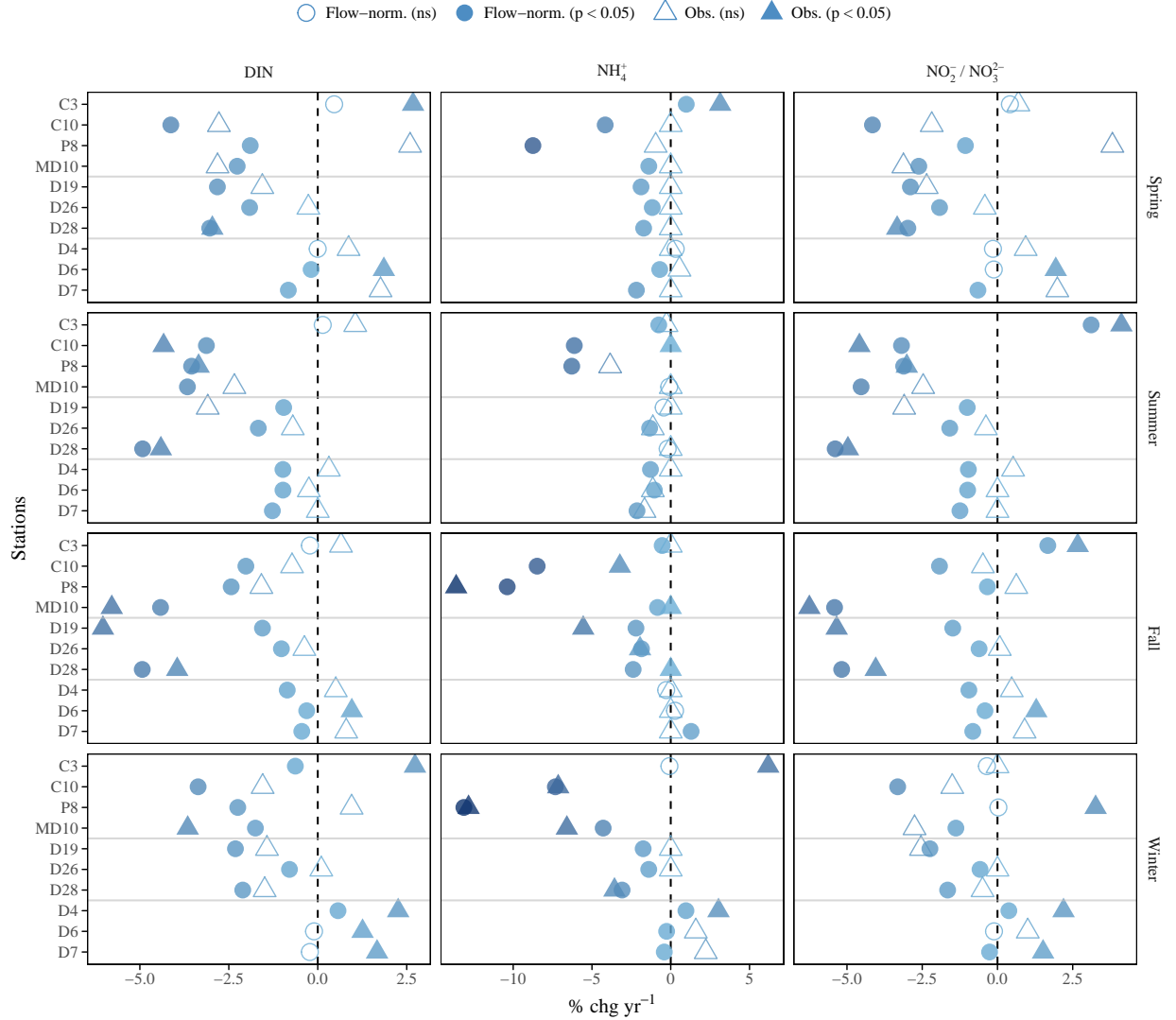


Figure S2: Results from seasonal Kendall tests on observed data (triangles) and flow-normalized predictions (circles) from WRTDS for nitrogen analytes. Results are shown as the percent change per year as the estimated Theil-Sen slope divided by the median for a given aggregation period (significance evaluated at  $\alpha = 0.05$ , based on  $\tau$ ). Trends are shown separately for different seasonal groupings from 1996-2013. Months for each season are Spring: MAM, Summer: JJA, Fall: SON, Winter: DJF. See Figure 3 for annual comparisons.

{fig:trndcc}

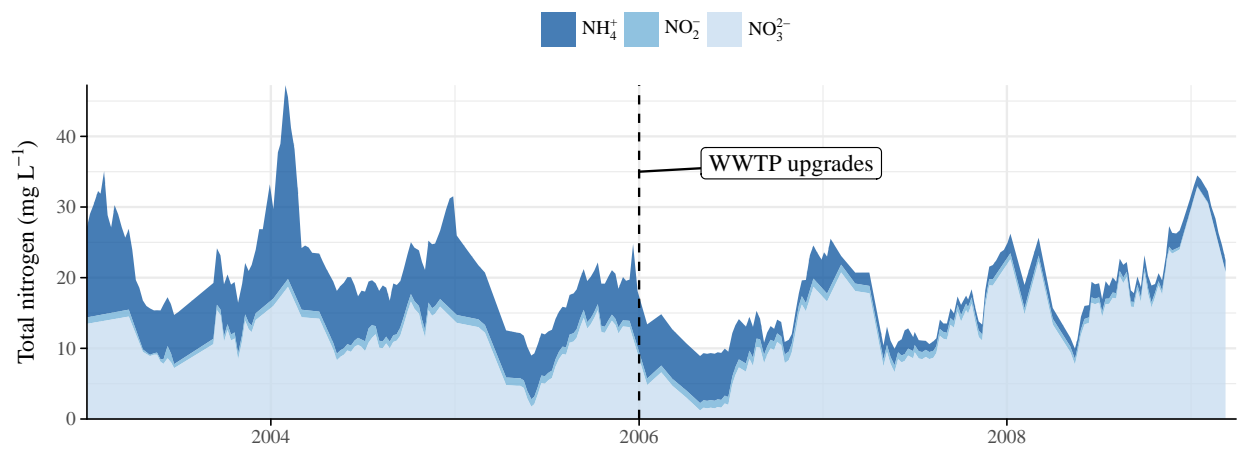


Figure S3: Nitrogen concentration measurements ( $\text{mg L}^{-1}$ ) from the City of Stockton Wastewater Treatment Plant, San Joaquin County. Wastewater discharge requirements were implemented in 2006 for nitrification/denitrification and tertiary filtration to convert ammonium to nitrate.

{fig:stock}